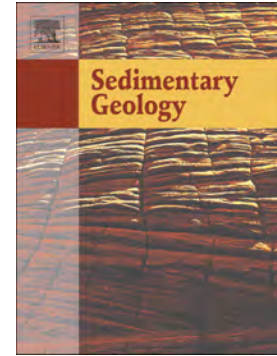


## Journal Pre-proof

Orbital cycles, differential subsidence and internal factors controlling the high-frequency sequence architecture in a sinemurian shallow carbonate platform (Mallorca Island, Spain)

Ana Sevillano, Beatriz Bádenas, Idoia Rosales, Antonio Barnolas, José María López-García



PII: S0037-0738(20)30144-5

DOI: <https://doi.org/10.1016/j.sedgeo.2020.105729>

Reference: SEDGEO 105729

To appear in: *Sedimentary Geology*

Received date: 6 May 2020

Revised date: 22 July 2020

Accepted date: 22 July 2020

Please cite this article as: A. Sevillano, B. Bádenas, I. Rosales, et al., Orbital cycles, differential subsidence and internal factors controlling the high-frequency sequence architecture in a sinemurian shallow carbonate platform (Mallorca Island, Spain), *Sedimentary Geology* (2020), <https://doi.org/10.1016/j.sedgeo.2020.105729>

This is a PDF file of an article that has undergone enhancements after acceptance, such as the addition of a cover page and metadata, and formatting for readability, but it is not yet the definitive version of record. This version will undergo additional copyediting, typesetting and review before it is published in its final form, but we are providing this version to give early visibility of the article. Please note that, during the production process, errors may be discovered which could affect the content, and all legal disclaimers that apply to the journal pertain.

***ORBITAL CYCLES, DIFFERENTIAL SUBSIDENCE AND INTERNAL  
FACTORS CONTROLLING THE HIGH-FREQUENCY SEQUENCE  
ARCHITECTURE IN A SINEMURIAN SHALLOW CARBONATE PLATFORM  
(MALLORCA ISLAND, SPAIN)***

Ana Sevillano <sup>a</sup>, Beatriz Bádenas <sup>b</sup>, Idoia Rosales <sup>c</sup>, Antonio Barnolas <sup>c</sup>, José María  
López-García <sup>a</sup>

<sup>a</sup> *Instituto Geológico y Minero de España (IGME), Felicià Fuster 7, 07006 Palma de  
Mallorca, Spain*

<sup>b</sup> *Departamento de Ciencias de la Tierra, Universidad de Zaragoza, Pedro Cerbuna  
12, 50009 Zaragoza, Spain*

<sup>c</sup> *Instituto Geológico y Minero de España (IGME), Ríos Rosas 23, 28003 Madrid,  
Spain*

\*Corresponding author. Tel: +34 971467020

E-mail address: [a.sevillano@igme.es](mailto:a.sevillano@igme.es)

**Abstract**

The ~125 m thick lower to lowermost upper Sinemurian peritidal to shallow subtidal platform carbonates in the Llevant Mountains of Mallorca (Spain) have been analysed from four stratigraphic sections, to provide new data on the hierarchical stacking pattern of high-frequency depositional sequences. Due to the fact that in shallow water environments the stacking of carbonate facies can be controlled by external (allocyclic) and internal (autocyclic) processes, deciphering the dominant controls on the high-

frequency sequence architecture of these platforms is a challenge. The studied carbonates encompass a high variety of facies representative of open lagoon, internal bars, restricted lagoon and tidal flats with local beach sands. Based on a detailed analysis of vertical facies trends and bounding surfaces, large-, medium- and small-scale sequences have been identified within the long-term transgressive-regressive facies cycle defined by the entire succession. Large-scale sequences (~10–30 m thick) and medium-scale sequences (~1–10 m thick) are generally shallowing-upward sequences bounded by sharp facies changes to relatively deeper facies, and have been related to sea-level variations driven by long- (~400 kyr) and short- (~100 kyr) eccentricity cycles respectively. The overprinting of differential subsidence (probably related to extensional tectonic) and carbonate production and accumulation processes varied throughout time, controlling the lateral continuity and preservation potential of the ~100 kyr medium-scale sequences. Shallowing-upward, locally aggradational, small-scale sequences (~0.3 to 5 m thick) are very variable in number and thickness and cannot be correlated between sections, pointing out that their most important controlling factor was the internal processes (hiatuses and erosion related to subaerial exposure at the peritidal caps, lateral migration of internal bars, local wave and currents patterns, depositional and erosional processes related to spring tides and storms) in the frame of a complex mosaic of facies within the studied platform.

**Key words:** *peritidal carbonate platform, high-frequency sequences, allocyclic and autocyclic factors, Sinemurian, Mallorca*

## 1. Introduction

The hierarchical stacking of high-frequency depositional sequences of different scales is very common in peritidal to shallow marine carbonate platform successions. Different

factors controlling sequence formation have been proposed, including: (a) sea level changes generated by insolation changes induced by orbital Milankovitch cycles (periodicities of ~20 kyr to ~400 kyr) (e.g., Strasser, 1991; D'Argenio et al., 1997; Strasser et al., 1999; Fischer et al., 2004; Preto et al., 2004; Husinec and Read, 2004; Sames et al., 2016); (b) changes in accommodation space due to synsedimentary tectonic activity and related subsidence (e.g., De Benedictis et al., 2007; Bosence et al., 2009); and (c) internal mechanisms, such as lateral migration of sedimentary bodies and changes in carbonate production rate and sediment transport direction (e.g., Ginsburg, 1971; Pratt et al., 1992; Wilkinson et al., 1999; Burgess, 2006; Yang et al., 2014; Kemp and Van Manen, 2019). The imprint of these allocyclic and autocyclic factors on the sedimentary cyclicity and, in particular, the influence of the orbital-induced sea-level variations, is often difficult to distinguish from each other (e.g., Goldhammer et al., 1993) due to the interplay of internal and external mechanisms in the sedimentary system, where the orbital signal is often not recorded, distorted and /or overprinted by local or regional tectonic subsidence and/or by internal variations of carbonate production, erosion and accumulation (Strasser et al., 1999; Zühlke, 2004; Bádenas et al., 2010; Strasser, 2018). In addition, local or regional tectonic subsidence and internal factors (e.g., hydrodynamic erosion/accumulation processes) act at different spatial and temporal scales compared to orbital cycles and control changes in time and space of accumulation (preservation) rates and, therefore, the preferential record of climate-controlled high-frequency sequences (e.g., Bádenas and Aurell, 2018). Moreover, the difficulties that arise in calibrating the time duration of the sedimentary cycles in shallow marine carbonate platform successions and in demonstrating their lateral continuity, hinder an unambiguous interpretation of their climate origin (e.g., Koerschner and Read, 1989; Zühlke et al., 2003; Preto et al., 2004).

The Lower Jurassic peritidal to shallow marine carbonate platform successions developed around the western Tethys usually display a hierarchical stacking of high-frequency depositional sequences that have been related to allocyclic and/or autocyclic mechanisms. In most of these platforms, a combination of factors controlling the cyclicity and the internal facies stacking has been suggested: orbital-driven sea-level changes, local or regional tectonic subsidence, and variations in local sediment supply and tidal flat progradation (Crevello, 1990, 1991; Walkden and De Matos, 2000; Bosence et al., 2000, 2009; Pomoni-Papaioannou and Kostopoulou, 2008; Pomoni-Papaioannou and Karakitsios, 2016; Bádenas et al., 2010; Aurell and Bádenas, 2015; Brandano et al., 2015; Belkhedim et al., 2019). Similar high-frequency depositional sequences have been described in the Sinemurian shallow platform successions of Mallorca (Es Barraca Member, Balearic Islands, Spain) (Barnolas and Simó, 1984; Sevillano et al., 2013). As has been described in earlier works (Barnolas and Simó, 1984; Prescott, 1988; Álvaro et al., 1989), the most prominent feature of these Sinemurian shallow subtidal to peritidal carbonates is the presence of m-scale shallowing-upward sequences. Sevillano et al. (2013) performed a detailed analysis of vertical facies trends and bounding surfaces in the type-locality of the Es Barraca Member, and identified a more complex sequential architecture from small-scale sequences (few m thick), to medium- and large-scale sequences (several tens of m), with the usual shallowing-upward, but also aggradational, facies trends. However, there is not detailed description of facies trends, vertical stacking patterns and lateral continuity of these high-frequency depositional sequences for the Sinemurian Balearic platform, nor is there an interpretation of the role of internal and external (climate, tectonic) controlling factors.

In this work, we study the hierarchical stacking of high-frequency sequences of different scales within a ~125 m thick succession of the lower Sinemurian to lowermost upper Sinemurian peritidal to shallow subtidal platform carbonates, belonging to the platform Stage-1 of the Es Barraca Member of Mallorca (sensu Sevillano et al., 2019). Identification and correlation of large-, medium- and small-scale sequences of four stratigraphic sections have been performed to illustrate temporal and spatial variations of high-frequency depositional sequences, and to decipher the possible interaction between orbital-driven sea-level variations, differential subsidence, and internal factors on carbonate production and accumulation processes controlling the hierarchical stacking and the character of these high-frequency depositional sequences.

## **2. Geological and stratigraphic setting of the study area**

The Balearic Islands in the western Mediterranean Sea have been considered as the northeastern extension of the Betic alpine orogenic belt (Azañón et al., 2002) (Fig. 1). According to recent palaeogeographic reconstructions, during the Jurassic the Balearic realm was located on the eastern margin of the Iberian Plate and to the southeast of the emergent Ebro High (Thierry, 2000; Scotese and Schettino, 2017) (Fig. 1A). Recently Etheve et al., 2018 showed the existence of a submerged Mesozoic rift basin between the Iberian Peninsula and the Balearic Islands, related to an early opening of the Gulf of Valencia. In this context the Jurassic of Mallorca would represent a southeastern margin of a segment of that Mesozoic basin. The opposing northwestern margin of this basin is partially located in the eastern Iberian Peninsula.

Mallorca is the largest island of the Balearic archipelago and includes three NE-SW oriented mountain ranges formed by preorogenic and synorogenic (Alpine) Mesozoic–Lower Cenozoic rocks (Tramuntana Range, Central Hills and Llevant Mountains),

which are surrounded by postorogenic Cenozoic and Quaternary sedimentary rocks (Palma, Inca-Sa Pobla and Campos basins) (Fig. 1B). The lowermost Jurassic sedimentary succession of Mallorca encompasses Hettangian coastal sabkha to restricted platform dolomites of the Mal Pas Formation. They are followed by Sinemurian shallow platform limestones (Es Barraca Member), lower Pliensbachian marls to open platform carbonates (Sa Moleta Member) and deltaic sandstones to conglomerates (Es Racó Member) of the Soller Formation, and finally upper Pliensbachian open sea shallow limestones of the Es Cosconar Formation (Álvaro et al., 1989; Rosales et al., 2018) (Fig. 1C). The Sinemurian succession of the Es Barraca Member studied here shows three successive stages of platform evolution with distinct facies associations and platform profiles (Sevillano et al., 2019): a broad, nearly-flat, peritidal to shallow subtidal platform during the early Sinemurian to earliest late Sinemurian (Stage-1); a muddy open platform during the late Sinemurian (Stage-2); and a peritidal to outer carbonate platform during the latest Sinemurian (Stage-3). These stages of platform evolution have transgressive and/or regressive facies trends (Sevillano et al., 2019), which are framed in the long-term Hettangian–Toarcian transgressive trend of western Europe (Hallam, 1989, 2001). The sedimentary evolution during the three stages proposed was controlled by the interplay between extensional tectonics related to Early Jurassic Tethyan rifting, the progressive platform flooding related to the Late Triassic–Early Jurassic global marine transgression and associated accommodation changes, and contemporaneous environmental perturbations (Sevillano et al., 2019).

This study is focused on the sequential architecture of the peritidal to shallow subtidal platform successions of the early Sinemurian to earliest late Sinemurian Stage-1 of the Es Barraca Member (Sevillano et al., 2019). It has been centred on four stratigraphic

sections located in the Llevant Mountains (Cutri, S'Heretat, Son Maina and Cuevas de Artà; Fig. 1B, C). The lower boundary of the studied Stage-1 is the contact with brecciated dolomites possibly belonging to the underlying Mal Pas Formation. This dolomitic unit is roughly attributed to the Hettangian (Álvaro et al., 1989) (Fig. 1C), although it is not precisely dated because of the lack of macro- and microfauna with biostratigraphic significance. Therefore, the position of the Hettangian-Sinemurian boundary in the study area is still uncertain. The top boundary of the Stage-1 is well preserved and exposed in the Cutri, S'Heretat and Son Maina sections. It appears as an abrupt change in sedimentation (deepening surface) between the studied peritidal to shallow subtidal platform successions of Stage-1 and the open carbonate platform facies (i.e., mudstones, skeletal wackestones and skeletal-oncolitic-peloidal wackestones-packstones) deposited in a muddy-dominated platform during the Stage-2 (Sevillano et al., 2019). In Cuevas the Artà section, the upper boundary is an unconformity represented by a ferruginous hardground overlain by Bajocian red nodular pelagic limestones with thin-shelled bivalves and ammonites (Álvaro et al., 1989; Sevillano et al., 2019). The thickness of Stage-1 (Fig. 2) is 122 m and 126 m in the most complete sections of Cutri and Son Maina respectively. The other two sections are incomplete. In S'Heretat section (70 m thick) the lower part of the succession is covered, whereas in Cuevas de Artà section (110 m thick) the succession is truncated on its top (Sevillano et al., 2019, 2020).

The foraminiferal assemblage in the Stage-1 of the Es Barraca Member shows the presence of *Siphovalvulina* sp., *Meandrovoluta asiagoensis* Fugagnoli and Rettori, *Glomospira* sp., *Mesoendothyra* sp., *Duotaxis* sp. and some textulariids in their lower part (Sevillano et al., 2019, 2020), which is compatible with an early Sinemurian age (Velić, 2007). The upper part of this Stage-1 shows in addition *Haurania* sp.,



*Everticyclammina praevirguliana* Fugagnoli and *Lituosepta recoarensis* Cati (Sevillano et al., 2019, 2020) that indicates a late Sinemurian age (Septfontaine, 1984; Boudagher-Fadel and Bosence, 2007; Velić, 2007; Fugagnoli and Bassi, 2015). A recent, detailed biostratigraphic analysis (Sevillano et al., 2020) has attributed the studied interval to the biozone A (*Siphovalvulina* sp. and *Mesoendothyra* sp. Interval Zone) and the base of the biozone B (*Lituosepta recoarensis* lineage Zone) of Septfontaine (1984) (Fig. 2). In Son Maina and S'Heretat sections the studied interval includes these two biozones, whereas in the Cuevas de Artà section only the Biozone A has been preserved below the hardground unconformity (Fig. 2). No detailed biostratigraphic data are available from the Cutri section due to an intense dolomitization of this succession (Fig. 2). Based on these biostratigraphic data, the duration of the studied interval would be estimated in ~ 4 Ma (following the chronostratigraphic chart by Ogg et al., 2016), if it is assumed that there are no major hiatuses within Stage-1 and that the entire lower Sinemurian and the lowermost upper Sinemurian are encompassed by the studied succession (Fig. 1C).

### 3. Methods

Platform carbonates of Stage-1 of the Es Barraca Member were logged bed-by-bed in Cutri, S'Heretat, Son Maina and Cuevas de Artà sections (Fig. 1C) for the characterization of facies trends, identification and correlation of the high-frequency sequences (Fig. 2). The facies characterization and facies associations of these peritidal to shallow subtidal platform successions has been already done by Sevillano et al. (2019), and just a brief summary of the main characteristics of the studied facies will be explained (see section 4.1).

The concept of high-frequency sequences of different scales is used here from a descriptive point of view, which implies a hierarchy of sequences in which smaller

sequences stack in longer sequences (e.g., Bádenas and Aurell, 2018). The identification of the different scale depositional sequences is based on two main criteria (e.g., Bosence et al., 2009; Bádenas et al., 2010): (1) the recognition of sequence boundaries, represented by discontinuity surfaces reflecting breaks in sedimentation, and (2) the vertical facies trends within sequences. Details of the criteria used for the identification and approximate age calibration of large-, medium- and small-scale sequences are included in section 5. As a general rule, large- and medium-scale sequences have a general vertical facies trends to shallower facies and are bounded by sharp surfaces associated with abrupt facies changes to relatively deep water facies. Small-scale sequences, which include subtidal facies shallowing up to intertidal-supratidal facies (with flat-pebble breccias, desiccation cracks, tepees), fit the classical peritidal cycles/sequences. Their sequence boundaries are well-marked, sharp bedding surfaces associated with a sharp facies change to subtidal facies, sometimes including evidences of reworking of previous semi-consolidated sediments (accumulation of black pebbles or lithoclasts of microbial laminites). Small-scale sequences that do not shallow up to tidal facies fit the subtidal cycles/sequences (*sensu* Osleger, 1991), sometimes without a sharp facies change at the sequence boundary, but just a prominent bounding surface reflecting submarine erosion or non-sedimentation (e.g., Bosence et al., 2009; Bádenas et al., 2010).

The physical tracing of the high-frequency sequences between logs is prevented due to the distance between sections (3 to 5 km for Cutri, S'Heretat and Cuevas de Artà; 25 km for Son Maina; Fig. 1A) and the absence of intermediate continuous outcrops.

Therefore, the correlation of large- and medium-scale sequences proposed here has been based on the best fit regarding facies trends recorded in the sequences, and considering the short distances (few km) between three of the four logs studied. The available recent

biostratigraphic data from benthic foraminifera of Sevillano et al. (2020) have also been taken into account for the correlation between sections, being aware of the existence of some uncertainty in the position of the limits between biozones A and B (Fig. 2), introduced by sampling bias and/or incompleteness of the fossil record.

## 4. Results

### 4.1. Summary of facies

The vertical and lateral facies distribution of the Stage-1 of Es Barraca Member in the four studied logs are included in Figure 2. Six main facies types representative of facies associations of tidal flat (facies 1–3), restricted lagoon (facies 4), internal bars and shoals (facies 5), and open lagoon (facies 6) environments were recognized by Sevillano et al. (2019). The conceptual depositional model proposed by these authors is represented in Figure 3 and selected images of facies are included in Figure 4.

The tidal flat environment encompasses two types of facies associations (Types 1 and 2 in Fig. 3). Type 1 tidal-flat facies association consists of four facies: supratidal flat-pebble breccia made of intraclasts of semi-consolidated laminated microbialites (facies 1A, Fig. 4a); supratidal microbial laminites with wavy-crinkled lamination (facies 1B, Fig. 4b); intertidal microbial laminites with parallel lamination (facies 1C, Fig. 4c); and intertidal fine-grained stromatolites (facies 1D). Type 2 tidal-flat facies association includes five facies: black-pebble conglomerates with pedogenic features (facies 2A) interpreted as formed in supratidal marsh areas with development of coastal soils; intertidal spongiostrome stromatolites with desiccation features (facies 2B, Fig. 4d); intertidal coarse-grained agglutinated stromatolites (facies 2C, Fig. 4e); mudstone with fenestral porosity formed in restricted ponds in the intertidal belt (facies 2D, Fig. 4f); and planar to cross-laminated intraclastic-peloidal and oolitic-peloidal grainstone with

vadose diagenetic features (facies 3, Fig. 4g), interpreted as deposits of local sandy beaches or as event beds (Sevillano et al., 2019).

The restricted lagoon environment (facies 4, Fig. 3) is represented by massive to slightly laminated mudstone to wackestone (facies 4A) with low fossil diversity (scarce ostracods, miliolids and other small benthic foraminifera), suggesting low-energy and fluctuations in sea-water salinity and/or temperature. It intercalates cm- to dm-thick beds of oolitic-peloidal-skeletal wackestone with parallel lamination (facies 4B), which represent episodic high-energy events, probably storms (Sevillano et al., 2019).

The inner bars and shoals environment (facies 5, Fig. 3) includes oolitic grainstone (facies 5A, Fig. 4h) and peloidal-foraminiferal grainstone (facies 5B, Fig. 4i), both with tractive structures (parallel and wavy lamination, normal grading, oriented bioclasts and intraclasts), indicative of moderate to high-energy conditions.

The open lagoon environment (facies 6, Fig. 3) consists of skeletal mudstone-wackestone to foraminiferal-peloidal-oncolitic wackestone to packstone (Fig. 4j-k). Common bioturbation, presence of lithic peloids, cortoids and oncoids, and high-diversity of skeletal components (fragments of bivalves, gastropods, dasycladalean algae, *Thaumatoporella parvovesiculifera*, *Cayeuxia* sp., echinoderm plates and benthic foraminifera; Fig 4j-k), suggest a shallow marine environment with normal marine salinity and long periods of quiet environmental conditions interrupted by occasional events of water agitation (Sevillano et al., 2019).

#### **4.2. High-frequency sequences**

The analysis of bounding surfaces and facies trends enables recognition of hierarchically stacked depositional sequences at three different scales within the

transgressive-regressive facies cycle defined in platform Stage-1 by Sevillano et al. (2019) (Fig. 2, Table 1): large-scale sequences (10 to 30 m thick, with average thickness of 16.5 m), medium-scale sequences (1 to 10 m thick, 4 m of average thickness) and small-scale sequences (0.3 to 5 m thick, with average thickness of 1 m).

#### 4.2.1 Large- and medium-scale sequences

A total of eight large-scale sequences (LS-1 to LS-8), each one including 3 to 5 medium-scale sequences, have been identified and correlated (Figs. 2, 5). Most of these correspond to shallowing-upward sequences bounded by sharp surfaces above, coinciding with abrupt facies changes to deeper water facies.

LS-1 has a lower contact covered in some sections and vague in others due to the uncertain contact with the underlying Hettangian dolomites. LS-1 has in all sections a general shallowing-upward facies trend from thick (aggradational) successions of restricted lagoon facies (4A: mudstone to wackestone) at its lower part, to predominant intertidal facies at the top (1C: microbial laminite; 2D: fenestral mudstone), alternating with minor amount of internal bars (5A: oolitic-peloidal grainstone and 5B: peloidal-intraclastic-foraminiferal grainstone) and restricted lagoon facies (4A: mudstone to wackestone) (Fig. 5). In Cutri and Son Maina sections, the upper boundary of LS-1 is a sharp deepening surface from intertidal facies to dominant shallow subtidal facies (inner bars, restricted lagoon) of the base of LS-2 (see also Fig. 2), whereas in Cuevas de Artà, this boundary is a sudden change to sand beach facies (3: intraclastic-peloidal and oolitic-peloidal grainstone). Five medium-scale shallowing-upward sequences from shallow inner platform to tidal flat facies, are clearly identified in Cutri section (1.1. to 1.5 in Fig. 5), whereas in Son Maina and Cuevas de Artà sections, only three shallowing-upward medium-scale sequences have been recognized (1.1 to 1.3, Fig. 5).

The top of the medium-scale sequence 1.1 roughly coincides with the boundary between the aggradational and the shallowing parts of LS-1 (Fig. 5). The shallowing interval of LS-1 has a variable number of medium-scale sequences, from 4 in Cutri (1.2 to 1.5), to 2 in Cuevas de Artà (1.2 and 1.3) and maybe 2 in Son Maina (1.2. and 1.3?), and therefore their correlation at this scale is uncertain.

LS-2 has a clear shallowing-upward trend in Cutri and Son Maina sections (Fig. 5). The lower part of the sequence is dominated by high-energy inner platform bars (5A: oolitic-peloidal grainstone, 5B: peloidal-intraclastic-foraminiferal grainstone) with minor intercalations of restricted lagoon facies (4A: mudstone to wackestone), intertidal facies (1C: microbial laminites; 2D: fenestral mudstone) and beach facies (3: intraclastic-peloidal and oolitic-peloidal grainstone). Within the upper part of the sequence there is an increase of restricted lagoon and inter- and supratidal flat facies, the latter including flat pebble breccia (1A). The Cuevas de Artà section includes a different suite of facies (Figs. 5, 6): beach facies 3, restricted lagoon facies 4 and thin levels of fenestral mudstones (2C) located at the base, passing upward to a thick succession dominated by beach facies 3 with minor intercalations of restricted lagoon facies 4 and intertidal stromatolites (2B and 2C), thus reflecting also a general shallowing upward trend. The upper boundary of LS-2 is a deepening surface from supratidal of wavy-crinkled microbial laminites (1B) and flat-pebble breccia (1A) in Cutri and Son Maina sections, and intertidal coarse-grained agglutinated stromatolite (2C) in Cuevas de Artà (Fig. 6), to subtidal restricted lagoon facies (4A) at the base of the LS-3. In these three sections, LS-2 is formed by 5 medium-scale sequences that have been proposed as correlatable considering the short distance (few km) between three of the four logs studied (2.1 to 2.5 in Fig. 5). These sequences display a shallowing-upward facies trend, from subtidal facies (inner bars and restricted lagoon) to tidal flat facies on top, and locally a

deepening-shallowing trend (e.g., medium-scale sequence 2.4 in Son Maina and Cuevas de Artà; Figs. 5, 6). It is interesting to notice that the 5 medium-scale sequences are recognizable in all sections despite the lateral variation in thickness of LS-2 (22.8 m in Cutri, 15.2 m in Son Maina and 28.6 m in Cuevas de Artà), although, the shallowing part of the LS-2 comprises the medium-scale sequences 2.4 and 2.5 in Cutri and Son Maina, while in Cuevas de Artà it starts at the upper part of medium-scale sequence 2.2 from which beach sand facies 3 dominates.

LS-3 has, in Cutri and Son Maina sections, a lower part with a predominance of restricted lagoon mudstones to wackestones (4A) with intercalated inner bars (5A and 5B) and intertidal microbial laminates (1C), and an upper part dominated by inter- and supratidal facies (1C, but also 2C: coarse-grained agglutinated stromatolites and 1A: flat-pebble breccia), thus reflecting a general shallowing-upward trend. In Cuevas de Artà section, LS-3 has a thin lower part with predominance of restricted lagoon facies 3 and a thick shallowing part dominated by tidal flat facies (2B and 2C: stromatolites; 2D: fenestral mudstone) and sand beach facies 3. The upper boundary of LS-3 is a sudden facies change from inter- and supratidal facies (e.g., flat-pebble breccia in Cutri section; Fig. 5) of the top of sequence LS-3 to relative deeper subtidal restricted lagoon facies (4A) of the base of LS-4. Four medium-scale sequences have been identified in LS-3 in all sections and have been considered as laterally continuous (3.1. to 3.4 in Fig. 5).

These sequences have a shallowing-upward facies trend from shallow subtidal facies to intertidal and occasionally supratidal facies on top, and are bounded by sharp bedding surfaces above which a facies shift to deeper water facies occur. Medium-scale sequences have been correlated despite the marked lateral variation in thickness of LS-3 (21.4 m in Cutri, 15.6 m in Son Maina and 32.8 m in Cuevas de Artà). In addition, like in LS-2, the shallowing part of the LS-3 sequence is initiated earlier in the thicker

Cuevas de Artà section (see predominance of tidal flat facies from the upper part of the medium-scale sequence 3.1), compared to the thinner Cutri and Son Maina sections, where the shallowing part comprises the medium-scale sequences 3.3 and 3.4.

LS-4 shows a shallowing-upward facies trend similar to that of LS-2 (Figs. 2, 5). The lower part of LS-4 has predominance of high-energy subtidal facies 5 (m-thick levels of peloidal-intraclastic-foraminiferal grainstone and oolitic-peloidal grainstone) alternating with restricted lagoon facies and minor tidal flat facies, whereas the upper part is characterized by the predominance of intertidal microbial laminites (1C), spongiostrome stromatolites (2B) and fenestral mudstones (2D), and supratidal flat-pebble breccia (1A) with subaerial exposure features (e.g., Son Maina and Cuevas de Artà sections). The top boundary of LS-4 is represented by a facies change from inter-supratidal facies to shallow-subtidal facies (restricted lagoon and internal bars) of the lowermost part of the overlaying LS-5. Five medium-scale sequences have been identified in LS-4 in all sections, then supporting their proposed lateral continuity (4.1 to 4.5, Fig. 5). Most of them show a shallowing-upward facies trend from subtidal to inter-and/or supratidal facies, although deepening-shallowing and possibly aggradational trends are also present (e.g., sequences 4.3, 4.4 and 4.5 in Son Maina section). It is interesting to note that, despite the lateral variation in thickness of LS-4 (14.2 m in Cutri, 17.8 m in S'Heretat, 10.8 m in Son Maina and 12.4 m in Cuevas de Artà), the medium-scale sequences are thought to be continuous and correlatable. The shallowing stage of the LS-4 starts in the medium-scale sequence 4.2 in Cutri and S'Heretat sections (see predominance of tidal flat facies), but its location in Son Maina and Cuevas de Artà is uncertain, due to the complex intercalation of facies. It has been tentatively located in the first beds of tidal flat facies in medium-scale sequence 4.1.



LS-5 displays variable facies trends in the four studied sections (Fig. 5). In Cutri and Cuevas de Artà sections, the sequence has a general aggradational trend where mudstone to wackestone of restricted lagoon (4A) alternate with intertidal parallel microbial laminites (1C), supratidal wavy-crinkled microbial laminites (1B) and occasionally supratidal flat-pebble breccia (1A). In S'Heretat section, LS-5 has a shallowing-upward trend, from a thin succession of subtidal inner bars facies (5B) and restricted lagoon facies (4A) at the lowermost part grading upward to a thick upper succession with a significant predominance of intertidal facies (2D: fenestral mudstone; 2B and 2C: spongistrome and fine-grained agglutinated stromatolites). In Son Maina section, the sequence shows also a general shallowing-upward trend with a thick lower part dominated by restricted lagoon facies (4A), which ends with open lagoon facies 6 (skeletal mudstone-wackestone to foraminiferal-peloidal-oncolitic wackestone to packstone) and a thinner upper part dominated by intertidal microbial laminites (1C) and internal bars (5B). The upper boundary of LS-5 has been placed in a facies change from inter-supratidal facies to low-energy shallow-subtidal facies (restricted lagoon, 4A) of the overlying LS-6 (Figs. 2, 5). LS-5 is highly variable in thickness (from 20.4 m to 12 m) and includes five medium-scale sequences in the thicker sections (5.1 to 5.5 in Cutri and Son Maina), but only three medium-scale sequences in the thinner sections (S'Heretat and Cuevas de Artà). Sequences 5.1 and 5.2 are shallowing-upward and can be well identified in Cutri, S'Heretat and Son Maina sections, but they probably merge into one shallowing-upward medium-scale sequence dominated by restricted lagoon facies in Cuevas de Artà section (see 5.1/2 in Fig. 5). Shallowing-upward sequences 5.3, 5.4 and 5.5 have been identified in Cutri and less clearly in Son Maina section. Only one shallowing-upward sequence dominated by inter- and supratidal facies is proposed as lateral equivalent of these sequences in S'Heretat (see 5.3/4/5 in Fig. 5). In Cuevas de

Artà, sequences 5.3 and 5.4 are merged into one shallowing-upward sequence 5.3/4, while sequence 5.5 can be well distinguished.

LS-6 has an almost homogeneous thickness and a general shallowing-upward facies trend in all sections, from a thin lower part dominated by restricted lagoon facies (4A) with discrete intercalations of internal bars (5B) and open lagoon facies 6 (e.g., Son Maina), to a thicker upper part with dominance of inter-supratidal facies, including wavy-crinkled microbial laminites (1B) and flat-pebble breccia (1A) in Cutri, and coarse-grained agglutinated stromatolites (2C) and fenestral mudstone (2D) in S'Heretat, Son Maina and Cuevas de Artà. The upper boundary of LS-6 is a sharp deepening from inter-supratidal microbial facies to open lagoon and locally restricted lagoon facies of the lower part of the overlying LS-7 (Fig. 5). This boundary is close to the boundary between the foraminifera biozones A and B recognized by Sevillano et al. (2020) in S'Heretat and Son Maina sections (Fig. 2). LS-6 includes two to four medium-scale sequences, showing shallowing-upward facies trends from inner platform to tidal flat facies (Fig. 5). Sequences 6.1 to 6.4 are identifiable and considered as correlatable one-by-one in Son Maina and Cuevas de Artà sections. However, only two medium-scale sequences are recognized in S'Heretat section, being the lower sequence 6.1/2/3 probably lateral equivalent of sequences 6.1, 6.2 and 6.3 of Son Maina and Cuevas de Artà sections. In Cutri section, three medium-scale sequences have been identified (6.1/2, 6.3 and 6.4; Fig. 5), the lower one considered as merged sequences 6.1 and 6.2. Despite the homogeneous thickness of LS-6 (around 12 m in all sections), the shallowing stage to inter-supratidal facies does not occur coevally in all sections (in medium-scale sequence 6.3 in Son Maina, and around the lowermost medium-scale sequence in the rest of the sections).

LS-7 is characterized by the dominance of open lagoon facies and includes four medium-scale sequences 7.1 to 7.4 in Cutri, Son Maina and S'Heretat with shallowing-upward and locally aggradational facies trends (e.g., 7.3 in Cutri section, Figs. 5, 7), which have been proposed as one-to-one lateral equivalent. LS-7 has a deepening-shallowing facies trend in all sections. In Cutri, the deepening part encompasses from medium-scale sequence 7.1 to the lower part of 7.4, and is indicated by the upward change from restricted lagoon facies (4A) with intercalated inter- and supratidal laminated microbial facies (1B and 1C) in 7.1 and 7.2, to a thick (~11 m) succession of restricted lagoon facies (4A and 4B) and internal bars (5B) in 7.3, that finishes with a m-thick level of subtidal open lagoon facies 6 of the lower part of 7.4. On top of this level there is a predominance of inter- and supratidal microbial facies, reflecting the shallowing stage of LS-7. In S'Heretat and Son Maina, the deepening part of LS-7 is characterized by open lagoon facies 6 with intercalated high-energy inner bars (5A: oolitic-peloidal grainstone) and restricted lagoon facies (4A). Open lagoon facies 6 are very thick in the medium-scale sequence 7.3 and the lowermost part of 7.4. The shallowing stage is indicated by the change from the open lagoon facies 6 to inter- and supratidal laminated microbial facies (1B and 1C) at the upper part of 7.4. The upper boundary of LS-7 is a facies change from inter- and supratidal facies (1B and 1C: microbial laminites; 1A: flat-pebble breccia) to restricted and open lagoon facies of the overlying LS-8 sequence. In Cuevas the Artà section, only the medium-scale sequence 7.1 is recorded, being its top truncated by an erosional unconformity covered by a ferruginous hardground surface overlain by Bajocian pelagic deposits (Álvaro et al., 1989; Sevillano et al., 2019, 2020). This observation is also coherent with the available biostratigraphic information that indicates the absence of the foraminiferal Biozone B in this section (Sevillano et al., 2020) (Fig. 2).

LS-8 is only recognized in Cutri, S'Heretat and Son Maina sections. Its upper boundary is the abrupt change between the here studied Stage-1 and the muddy carbonate platform succession of the Stage-2 of the Es Barraca Member (Sevillano et al., 2019) (Fig. 1C). The thickness and the number of preserved medium-scale sequences in the LS-8 is highly variable. LS-8 displays a shallowing-upward facies trend in the Cutri section and an aggradational facies trend in S'Heretat. In these two sections only one medium-scale sequence is preserved. In Son Maina, the thickest section, LS-8 shows an aggradational facies trend including three shallowing-upward medium-scale sequences (8.1 to 8.3 in Fig. 5) with alternating open lagoon and restricted lagoon facies at their bases and some few intercalations of thin (cm-thick) beds of intertidal microbial laminites on top (Fig. 5).

#### 4.4.2. Small-scale sequences

The small-scale sequences are the elementary sequences recognized in the studied successions based on the following criteria: (1) the presence of sharp bedding planes, which can coincide or not with a vertical change of facies; and (2) the vertical facies trends, when present (Figs. 5–7; e.g., Bosence et al., 2009; Bádenas et al., 2010). Small-scale sequences range between 0.3 to 5 m in thickness, with 1 m in average, and are usually shallowing-upward and occasionally aggradational encompassing only one facies (Table 1, Figs. 5–7). Small-scale sequences with aggradational trend involve only one facies type and are common in subtidal restricted lagoon, internal bars and open lagoon facies (e.g., small-scale sequences in medium-scale sequences 1.1 and 2.3 in Cutri, and in 7.2 and 7.3 in Son Maina, Fig. 5), but can also involve only intertidal facies (e.g., small-scale sequences in 6.1/2/3 in S'Heretat, Fig. 5).

Shallowing-upward small-scale sequences are either subtidal or peritidal sequences, usually including part, but not all the facies representative of the different depositional environments, from open lagoon or high-energy subtidal facies to restricted lagoon and to intertidal and/or supratidal facies (see all different cases in Fig. 8). Based on analysis of the elementary sequences along the four studied sections and the facies trends recorded, two types of idealized shallowing-upward small-scale sequences can be proposed (Fig. 8). Both have subtidal open lagoon facies at the bottom followed upward by subtidal oolitic and peloidal internal bars, restricted lagoon facies and finally peritidal caps, but differ in the nature of the peritidal caps. One includes facies of Type 1 tidal-flat facies association with intertidal fine-grained stromatolites (1D) and parallel microbial laminites (1C), and supratidal wavy-crinkled microbial laminites with tepees (1B) and flat-pebble breccias (1A) at top, indicative of desiccation during subarerial exposure. The other shows facies of Type 2 tidal-flat facies association, with sand beach grainstones with pendant cementation (3), mudstones with fenestral porosity formed in restricted ponds in the intertidal environment (2D), intertidal spongiostrome and agglutinated stromatolites (2C and 2B) and black-pebble conglomerates indicative of pedogenic caps (2A).

As shown in Figure 8, in the studied sections there is a high variability of thickness and facies stacking of the small-scale sequences. In particular, most of the shallowing-upward sequences recorded show gradual facies changes, following the pattern of the idealized small-scale sequences. However, occasional peritidal sequences with internal sharp facies changes are also recorded, mainly related to the presence or absence of internal bars, which represent discontinuous sedimentary bodies within the studied platform (Fig. 2). In addition, the number of small-scale sequences within the medium-scale sequences is highly variable (from 1 to 17: Table 1), and also laterally from log to

log in the same medium-scale sequence (see red numbers in Fig. 5; e.g., medium-scale sequence 3.1 has 1, 4 or 5 small-scale sequences).

## 5. Discussion

### 5.1. Large- and medium-scale sequences: eccentricity cycles with overprinting of differential tectonic subsidence

The overall vertical facies distribution of the peritidal to shallow subtidal platform carbonates of the early Sinemurian to earliest late Sinemurian Stage-1 of the Es Barraca Member reflects a long-term transgressive (deepening) trend followed by a short regressive (shallowing) interval that conforms a long-term T-R facies cycle (Sevillano et al., 2019) (Fig. 2). The long-term transgressive facies trend of the T-R facies cycle is indicated by a predominance of supra- and intertidal flat facies alternating with restricted lagoon and internal bars facies at the lower part, followed upward by a gradual increase in the proportion of subtidal open lagoon facies 6. The maximum flooding interval has been placed at the maximum accumulation of these open lagoon facies, which occurs in the middle part of the large-scale sequence LS-7 in all sections (except in the Cuevas de Artà section where this part of the succession was eroded away before the Bajocian; Figs. 2, 5). The regressive facies trend of the T-R facies cycle is reflected by the rapid upward increase in the accumulation of tidal flat deposits, accompanied by restricted lagoon facies and internal bars.

This long-term T-R facies cycle encompasses eight large-scale sequences (10–30 m thick), each one including an average number of four medium-scale sequences (1–10 m thick; Fig. 5, Table 1). Considering the uncertainty of the time duration of the studied long term T-R facies cycle (~ 4 Ma following Ogg et al., 2016, chronostratigraphy; Fig. 1), and that of ancient Milankovitch cycle periods (e.g., Waltham, 2015) the average

time duration of large-scale sequences would be close to that of the long eccentricity cycles (~400 kyr) and, based on the observed mean 1:4 relationship of the large- and medium-scale sequences (e.g., Strasser et al., 2006), the medium-scale sequences would fit the short eccentricity (~100 kyr) cycles. Eccentricity-related sequences in the greenhouse Jurassic climate mode recorded in similar Jurassic shallow-platform successions have been interpreted as reflecting climate-driven, low amplitude sea-level variations (e.g., Crevello, 1991; Strasser et al., 1999; Aurell and Bádenas, 2004; Colombié and Strasser, 2005; Brandano et al., 2015; Pomoni-Papaioannou and Karakitsios, 2016; Strasser, 2018). In particular, in the Lower Jurassic successions of the High Atlas Crevello (1991) recognized bundles of elementary cycles, similar to the medium-scale sequences proposed here, which were driven by short eccentricity-related sea-level variations with amplitude of around 5 m. In the Apennines, Brandano et al. (2015) also recognized superbundles and bundles of elementary cycles, similar to the large- and medium-scale sequences described here (Table 2).

In the studied case, most of the described large-scale sequences correspond to shallowing-upward sequences bounded by deepening (flooding) surfaces (Fig. 2), thus indicating that carbonate production and accumulation rates were high enough to fill the accommodation space created by the long eccentricity-related sea-level variations and subsidence. The only exception is LS-7 which is a deepening-shallowing upward sequence, whose deepening stage roughly coincides with the maximum flooding interval of the long-term T-R facies cycle. The presence of this deepening stage in LS-7 can be explained as the modulation of long eccentricity-related sea-level variations by the long-term sea-level rise of this larger-scale T-R cycle, as deepening intervals in shorter scale-sequences have more potential to develop during the deepening stage of larger-scale sequences (e.g., Colombié and Strasser, 2005).

The thicknesses and sedimentary trends of the large-scale sequences (~400 kyr) and the number and facies trends of the medium-scale sequences (~100 kyr) included in them can vary laterally even between relative close sections (e.g., LS-5 in Cutri and S'Heretat, which are 5 km apart, although in different structural units). This reflects the complex overprinting of differential subsidence and carbonate production upon the orbital-driven sea-level variations. In particular, the comparison of the number of medium-scale sequences with the accumulation rates deduced for the large-scale sequences could be explained by the following cases or scenarios (Fig. 9):

Case 1: the number of medium-scale sequences within a large-scale sequence is constant in all sections, despite lateral variation in accumulation rate of the large-scale sequence. This occurs in LS-2 (accumulation rate of 3.8–7 cm/kyr), LS-3 (3.9–8.2 cm/kyr), LS-4 (2.8–4.8 cm/kyr) and LS-7 (4.7–7.8 cm/kyr), all of them including 4 to 5 correlatable medium-scale sequences (Fig. 9). This indicates that, at least for LS-2, LS-3, LS-4 and LS-7, the accommodation changes driven by eccentricity-related sea-level variations dominated over other controlling factors such as differential subsidence and changes in sedimentary rates. The slight mismatch in the position of the shallowing stages of the large-scale sequences LS-2, LS-3 and LS-4 among sections (Fig. 9) can be interpreted as reflecting the overprint of internal factors, such as changes in carbonate production, accumulation, and accommodation between sections. For example, shallowing in LS-2 and LS-3 starts earlier in the thicker Cuevas de Artà section characterized by the predominance of inter-supratidal facies (Fig. 5), thus indicating that in this section high peritidal carbonate accumulation compensated high rates of accommodation. Differential subsidence can be also deduced if comparing the proposed correlation of medium-scale sequences of LS-2, LS-3, LS-4 and LS-7 (Figs. 5, 9). Most of these sequences are shallowing-upward, thus reflecting that high accumulation



compensated accommodation, even in areas of higher subsidence (e.g., medium scale-sequence 3.4 in Cuevas de Artà, Fig. 5). The local presence of aggradational and deepening-shallowing trends in medium scale-sequences is mainly linked to lagoon facies and can be interpreted as reflecting lateral variations in production/accumulation in this wide depositional environment. In the case of local aggradational trend of the medium-scale sequence 7.3 (Fig. 5), the overprinting of larger-scale accommodation (i.e., deepening stage of LS-7 plus maximum flooding interval of the long-term T-R facies) on the sedimentary trend of the short eccentricity-related medium-scale sequence, cannot be discharged.

Case 2: The number of medium-scale sequences within a large-scale sequence varies along section, coinciding with the lateral variation in accumulation rates of the large-scale sequence. This occurs in LS-5 and LS-8 (Fig. 9). In LS-5, five medium-scale sequences can be recognized in areas of higher accumulation (Cutri and Son Maina sections), but only three medium-scale sequences in areas of lower accumulation and presumably less subsidence (S'Heretat and Cuevas de Artà). This suggests that in these sections the missing sequences did not accumulate or are amalgamated. A similar situation is observed in sequence LS-8, which has 3 sequences in the more subsiding Son Maina section, whereas in less subsiding areas (Cutri and S'Heretat) the entire LS-8 and therefore their medium-scale sequences, are very reduced, likely because they pinch out, are eroded or are amalgamated. Both cases indicate that accommodation changes driven by short eccentricity-related sea-level variations were obscured by other factors (subsidence, sedimentary rates, type of sedimentary production, water depth of the depositional environment, etc.) that produced differential accumulation rates among sections. In particular, sequence architecture in LS-5 and LS-8 conforms to the model of Bádenas et al. (2010) for the preservation potential of climate-driven sequences

modulated by subsidence, with merging of sequences in areas of lower accommodation space.

Case 3: The number of medium-scale sequences within a large-scale sequence varies among sections, despite there is a homogeneous and low accumulation rate of the large-scale sequence. This occurs in LS-6 that has a lower accumulation rate (2.3–3.1 cm/kyr) compared with other large-scale sequences, and includes 2 to 4 medium-scale shallowing-upward sequences (Fig. 9). This case conforms the proposed model by Bádenas and Aurell (2018) of low preservation potential of short eccentricity-related medium-scale sequences in shallow settings with low accumulation rates, due to the combination of low accommodation and effectiveness of the erosional processes in these settings. Also the definition of medium-scale sequences may be obscured (amalgamated) in areas without facies variability and frequent presence of erosional surfaces, like in the case of the inter-supratidal dominated S'Heretat section (Fig. 9).

In summary, there is a complex interaction between orbital-driven sea-level variations, differential subsidence, carbonate production and accumulation, controlling the number and lateral continuity of the medium-scale sequences, including a predominant control of short eccentricity (100 kyr)-driven sea-level variations (Case 1) and differential subsidence (Case 2) plus internal process like erosion (Case 3) influencing their preservation potential.

Therefore, a probably combination of tectonically and orbitally driven accommodation changes controlled the generation of medium-scale sequences of the studied early Sinemurian to earliest late Sinemurian platform Stage-1. This interaction has also been described in other Lower Jurassic peritidal and shallow carbonate platforms of the western Tethys (Iberian and Betic Ranges, Spain, Bosence et al. 2000, 2009, Bádenas et

al. 2010; High Atlas, Morocco, Crevello 1991; Central Apennines, Italy, Brandano et al. 2015; Central western Creta; Greece, Pomoni-Papaioannou and Kostopoulou, 2008, Pomoni-Papaioannou and Karakitsios, 2016; Dorsales, Tunisia, Bosence et al, 2009; Traras Mountains, Algeria, Belkhedim et al, 2019) where cycles or sequences similar to our medium- and large-scale sequences have been interpreted as a result of local or regional tectonic subsidence and orbitally driven sea level variations (Table 2). In Mallorca island a clearer influence of tectonic activity has been deduced for the overlaying late Sinemurian platform Stage-2 (Sevillano et al. 2019). These authors observe, since the stage-2, local slumps indicative of tectonic instability controlling the change of depositional gradient and platform profile, all this in relation with the initial extensional tectonic phases related to early Jurassic Tethyan rifting. Our results point out that probably this extensional tectonic activity already started during the early Sinemurian.

## **5.2. Small-scale sequences: dominant imprint of internal process**

### **5.2.1. Time calibration of small-scale sequences**

The origin of the small-scale (elementary) sequences recorded (Fig. 8) can be interpreted in relation to allocyclic processes (orbital-driven sea-level changes, tectonics) and/or autocyclic processes (e.g., Colombié and Strasser, 2005). Time calibration of these sequences can be used to discuss their possible allocyclic nature. Assuming an average duration of ~100 kyr for the medium-scale sequences, and taking into account the number of small-scale sequences within each medium-scale sequences, the following trends in cases 1 to 3 explained above can be deduced (Figs. 5, 9):

Case 1: In large-scale sequences LS-2, LS-3, LS-4 and LS-7, formed by four or five medium-scale sequences (~100 kyr), the resulting average duration of small-scale

sequences is highly variable, ranging from ~5.8 to ~100 kyr. The highest mean value of ~100 kyr derives from the fact that some of the medium-scale sequences include (or coincide with) only a small-scale sequence (e.g., medium-scale sequences 4.2 to 4.5 in Cutri section or 4.4 and 4.5 in S'Heretat section; Fig. 5). However, the small-scale sequences with average duration of ~20 kyr (duration close to precession cycles) could be considered preferentially developed in areas with higher accumulation rates (presumably more subsident), but not in areas with lower accumulation rates.

Cases 2 and 3: For the large-scale sequences LS-5 and LS-6, with a variable number (from 2 to 5) of medium-scale sequences (~100 kyr), the average duration of the small-scale sequences is also highly variable (~9 to ~100 kyr). Nevertheless, in LS-5, with lateral variation of accumulation rate, the average duration of some of the small-scale sequences is close to ~20 kyr in areas with higher sediment accumulation, and probably greater subsidence (e.g., Cutri and Son Maina; Fig. 9). Values close to ~20 kyr are also observed but randomly distributed in the medium-scale sequences of the large-scale sequence LS-6, characterized by uniform but low accumulation rate.

In summary, in all the large-scale sequences the resulting time duration of the small-scale sequences is highly variable (from ~5.8 to ~100 kyr). Some of the small-scale sequences could fit the duration of precession cycles of the Milankovitch frequency band (~20 kyr), but they do not have a well-defined pattern of distribution. The observed randomness in duration and distribution of these small-scale sequences could point out that probably their relation with orbital (precession) signal is not very confident at this scale, and if present, it would be mainly overprinted by internal and other external factors. Tectonic subsidence could control the better preservation of precession-related small-scale sequences in areas of higher subsidence. However, as a whole, the variability in the estimated time duration of small-scale sequences, thickness,

and facies stacking (Fig. 8) indicate a strong imprint of autocyclic processes inherent to the sedimentary system (e.g., progradation of tidal flats, Ginsburg, 1971; Belkhedim et al., 2019; lateral migration of sedimentary bodies and local erosional processes, Pratt and James, 1986; Strasser 1991). For example, if the small-scale sequences culminate with subaerial exposure at the sequence boundary, as is the case of peritidal small-scale sequences recorded here (Fig. 8), the time of non-deposition or erosion involved in the sequence boundary can be longer than 20 kyr (Sadler, 1981, 1994), resulting in “missed beats” in the cyclostratigraphic record (Belkhedim et al., 2019; Strasser, 2019). In other cases, facies such as high-energy oolitic bars can migrate laterally within the inner platform or be displaced during events such as storms or spring tides (e.g. Hine, 1977; Sapraks and Rankey, 2013) , generating erosional processes and giving rise to small-scale sequences with internally sharp facies changes (Fig. 8), therefore representing autocyclic sequences. For these reasons (their variable facies stacking and possible existence of laterally discontinuous bounding exposure surfaces; e.g., Manifold et al., 2020), the identification and correlation of this small-scale sequences in shallow water successions becomes very difficult.

### **5.2.2. Precession cycles in facies mosaic**

Sevillano et al. (2019) interpreted the development of the peritidal carbonate facies of the Es Barraca Member as a facies mosaic with poorly structured facies belts (Fig. 2), similar to that of some Holocene peritidal systems (e.g., Berkeley and Rankey, 2012). In this type of coastal environments, even a sea-level change of some few tens of centimeters will induce important changes in the distribution of tidal channels, microbial mats, small ponds and levees. Also depositional and erosional processes related to storms and spring tides are frequent (i.e., controlling lateral shift of internal bars or producing multiple erosion surfaces within intertidal sediments; Prados and

Bádenas, 2015). All these autogenic processes (spatially self-organizing processes sensu Pursik et al., 2016) can be the dominant factor in generating the cyclicity (e.g., Manifold et al., 2020) and/or can hide the external controlled sea-level signal on the development of sedimentary sequences (Dexter et al., 2009; Bádenas and Aurell, 2018), especially those of short time duration (e.g., precession cycles).

Indeed, in this type of environment, climate and/or tectonic driven accommodation changes of different time duration, and the complex interaction of internal and external factors on carbonate production/accumulation (Strasser, 2018; Bosence et al., 2009; Bádenas et al., 2010), are expected to have a complex impact on the resulting facies stacking of the elementary (small-scale) sequences potentially related with precession cycles. Even in orbital-driven small-scale sequences, shallowing-upward, aggradational or deepening-upward trends can develop contemporaneously in different sections depending on their position on the platform and the relationship between sea-level changes and the accumulation potential (Strasser, 2018). As a result, a regular pattern of facies trends within the small-scale sequences has been really difficult to find, as is the case of the varied facies trends recorded in the small-scale sequences of the studied platform succession (Figs. 5, 8). This variety in facies trends and the fact that almost any individual small-scale sequences can be correlated laterally across sections point out that they cannot be interpreted unequivocally as a precession-related sequences, and so internal processes, in the frame of a complex mosaic of facies within the studied platform, were the most important factor controlling the nature and number of small-scale sequences, rather than the allocyclic (orbital) signal and/or tectonic driven accommodation changes.

## **6. Conclusions**

Identification and correlation of large-, medium- and small-scale sequences of Sinemurian carbonates in four stratigraphic sections located in the Llevant Mountains of Mallorca (Balearic Island, Spain) have been undertaken to elucidate the factors controlling the hierarchical stacking pattern of the high-frequency depositional sequences and their internal facies organization. The main conclusions can be summarized as follows:

1. The internal processes in the frame of a complex mosaic of facies from open lagoon to tidal flats were the main factors controlling the high lateral variability in the number and facies stacking pattern of small-scale sequences, rather than a possible, but not likely, dominance of the orbital signal (precession cycles) and tectonic driven accommodation changes. Internal factors that controlled this heterogeneity include hiatuses and erosion related to subaerial exposure at the peritidal caps, lateral migration of facies like internal bars, local wave and currents patterns, depositional and erosional processes related to spring tides and storms, etc.
2. Long- and short-eccentricity related sea-level changes were the dominant control of the large- and medium-scale sequences respectively, with probably local extensional tectonics (differential subsidence) controlling the preservation potential of short-eccentricity related medium-scale sequences (i.e., merging of sequences in areas of lower accommodation space). A variable imprint through time of the differential subsidence among sections has probably been recorded, related to the onset of the synsedimentary tectonics, in the context of the initial phases of extensional tectonics related to Early Jurassic Tethyan rifting.
3. Accommodation for the large-scale sequences was also modulated by the long term sea-level T-R facies cycle of the early-earliest late Sinemurian. Most of the

large-scale sequences are shallowing-upward, thus indicating that carbonate sedimentation was high enough to fill the accommodation space created by both the long eccentricity-related sea-level variations and the long-term relative sea level. The only exception is the deepening-shallowing upward large-scale sequence LS-7, whose deepening interval was developed around the maximum flooding interval of the long-term T-R facies cycle, increasing therefore its expression. The decrease in the accommodation space during the short and sharp regressive phase of the long term T-R facies cycle controlled the poor development of sedimentary thickness of its large-scale sequence (LS-8), resulting in minimum accumulation, probably local erosion and merging of its medium-scale sequences in areas of lower accommodation space.

The analysis of the origin of the high-frequency sequences in shallow carbonate platforms is not an easy task because it requires understanding the complex interaction of allocyclic (tectonic, climate) factors and autocyclic processes inherent in these environments. The results presented here emphasize the fact that that complexity also derives from the different temporal and spatial scales of these processes: from local, short time and non-periodic autocyclic process, to local-regional, non-periodic extensional tectonics, to global and periodic orbitally driven climate changes. In particular, for the studied case the interaction of tectonics and climate in generating accommodation changes also varied throughout time because its context within the initial extensional tectonic phases related to early Jurassic Tethyan rifting.

### **Acknowledgements**

This paper is a contribution to the research projects RTI2018-093613-B-100 and CGL2017-85038-P funded by the Spanish Ministry of Science, Innovation and



Universities, and Government of Aragón-FEDER 2014e2020 (Group E18, Aragosaurus. Recursos Geológicos y Paleoambientales). The authors acknowledge an anonymous reviewer, Marco Brandano and editor Jasper Knight, whose comments and suggestions improved the original version of the manuscript.

## References

Álvaro, M., Barnolas, A., Cabra P., Comas-Rengifo, M.J., Fernández-López, S.R., Goy, A., Del Olmo, P., Ramírez del Pozo, J., Simó, A., Ureta, S., 1989. El Jurásico de Mallorca (Islas Baleares). Cuadernos de Geología Ibérica 13, 67–120.

Aurell, M., Bádenas, B., 2004. Facies and depositional sequence evolution controlled by high-frequency sea-level changes in a shallow-water carbonate ramp (late Kimmeridgian, NE Spain). Geological Magazine 141, 717–733.

Aurell, M., Bádenas, B., 2015. Análisis comparado de secuencias de alta frecuencia en plataformas carbonatadas con subsidencia diferencial (Sinemuriense, Cordillera Ibérica). Revista de la Sociedad Geológica de España 28, 77–90.

Azañón, J.M., Galindo-Zaldivar J., García-Dueñas, V., Jabaloy, A., 2002. Alpine Tectonics II: Betic Cordillera and Balearic Islands. In: Gibbons, W., Moreno, T. (Eds), The Geology of Spain, Geological Society of London Special Publication, pp. 401–416.

Bádenas, B., Aurell, M., Bosence, D., 2010. Continuity and facies heterogeneities of shallow carbonate ramp cycles (Sinemurian, Lower Jurassic, North-east Spain). Sedimentology 57, 1021–1048.

- Bádenas, B., Aurell, M., 2018. The down-dip preferential sequence record of orbital cycles in greenhouse carbonate ramps: examples from the Jurassic of the Iberian Basin (NE Spain). In: Montenari, M. (Ed), *Stratigraphy and timescales 3*. Elsevier, Amsterdam, pp. 285–325.
- Barnolas, A., Simó, A., 1984. In: Barnolas, A. (Ed.), *Sedimentología del Jurásico de Mallorca*. Grupo Español del Mesozoico, IGME-CGS, Madrid, pp. 263.
- Berkeley, A., Rankey, E.C., 2012. Progradational Holocene carbonate tidal flats of Crooked Island, south-east Bahamas: An alternative to the humid channelled belt model. *Sedimentology* 59, 1902–1925.
- Boudagher-Fadel, M., Bosence, D.W.J., 2007. Early Jurassic benthic foraminiferal diversification and biozones in shallow-marine carbonates of western Tethys. *Senckenbergiana Lethaea* 87, 1–39.
- Bosence, D.W.J., Wood, J., Rose, E.P.F., Qing, H., 2000. Low- and high frequency sea-level changes control peritidal carbonate cycles, facies and dolomitization in the Rock of Gibraltar (Early Jurassic, Iberian Peninsula). *Journal of the Geological Society of London* 157, 61–74.
- Bosence, D.W.J., Procter, E., Aurell, M., Bel Kahla, A., Boudagher-Fadel, M., Casaglia, F., Cirilli, S., Mehdie, M., Nieto, L., Rey, J., Scherreiks, R., Soussi, M., Waltham, D., 2009. A tectonic signal in high-frequency, peritidal carbonate cycles? A regional analysis of Liassic platforms from western Tethys. *Journal of Sedimentary Research* 79, 389–415.

Brandano, M., Corda, L., Tomassetti, L., Testa D., 2015. On the peritidal cycles and their diagenetic evolution in the lower Jurassic carbonates of the Calcare Massiccio formation (central Apennines). *Geologica Carpathica* 66, 393–407.

Burgess, P.M., 2006. The signal and the noise: Forward modelling of allocyclic and autocyclic processes influencing peritidal stacking patterns. *Journal of Sedimentary Research* 76, 962–977.

Colombié, C., Strasser, A., 2005. Facies, cycles, and controls on the evolution of a keep-up carbonate platform (Kimmeridgian, Swiss Jura). *Sedimentology* 52, 1207–1228.

Crevello, P., 1990. Stratigraphic evolution of Lower Jurassic carbonate platforms: record of rift tectonics and eustasy, central and eastern High Atlas, Morocco [Ph.D. Dissertation]. Colorado School of Mines, Golden, Colorado, pp. 456.

Crevello, P.D., 1991. High-frequency carbonate cycles and stacking patterns: Interplay of orbital forcing and subsidence on Lower Jurassic rift platforms, High Atlas, Morocco. In: Franseen, E.K., Watney, W.L., Kendall, C.G.St.C., Ross, W. (Eds), *Sedimentary Modeling: Computer Simulations and Methods for Improved Parameter Definition*. Kansas Geological Survey Bulletin 233, pp. 207–230.

D'Argenio, B., Ferreri, V., Amodio, S., Pelosi, N., 1997. Hierarchy of high-frequency orbital cycles in Cretaceous carbonate platform strata. *Sedimentary Geology* 113, 169–193.

De Benedictis, D., Bosence, D.W.J., Waltham, D.A., 2007. Tectonic control of peritidal carbonate parasequence formation: an investigation using forward tectonostratigraphic modelling. *Sedimentology* 54, 587–605.

Dexter, T.A., Kowalewski, M., Read, F.F., 2009. Distinguishing Milankovitch Driven Processes in the Rock Record from Stochasticity Using Computer Simulated Stratigraphy. *The Journal of Geology* 117, 349–361.

Etheve, N., Mohn, G., Frizon de Lamotte, D., Roca, E., Tugend, J., Gómez-Romeu, J., 2018. Extreme Mesozoic Crustal Thinning in the Eastern Iberia Margin: The Example of the Columbrets Basin (Valencia Trough). *Tectonics* 37, 1–27.

Fischer, A.G., D'Argenio, B., Silva, I.P., Weissert, H., Ferreri, V., 2004. Cyclostratigraphic approach to Earth's history: an introduction. In: D'Argenio, B., Fischer, A.G., Premoli Silva, I., Weissert, H., Ferreri, V. (Eds), *Cyclostratigraphy Approaches and Case Histories*. SEPM Special Publications 81, pp. 5–16.

Fugagnoli, A., Bassi D., 2015. Taxonomic and biostratigraphic reassessment of *Lituosepta recoarensis* Cati, 1959 (foraminifera, lituolacea). *Journal of Foraminiferal Research*, 45, 4, 402–412.

Ginsburg, R.N., 1971. Landward movement of carbonate mud: new model for regressive cycles in carbonates (abstract). *American Association of Petroleum Geologists Bulletin* 55, 340.

Goldhammer, R.K., Lehmann, P.J., Dunn, P.A., 1993. The origin of high-frequency platform carbonate cycles and third-order sequences (Lower Ordovician El Paso Gp, West Texas); constraints from outcrop data and stratigraphic modeling. *Journal of Sedimentary Research* 63, 318–359.

Hallam, A., 1981. A revised sea-level curve for the early Jurassic. *Journal of the Geological Society of London* 138, 735–743.

Hallam, A., 2001. A review of the broad pattern of Jurassic sea-level changes and their possible causes in the light of current knowledge. *Palaeogeography, Palaeoclimatology, Palaeoecology* 167, 23–37.

Husinec, A., Read, J.F., 2018. Cyclostratigraphic and  $\delta^{13}$  record of the lower Cretaceous Adriatic platform, Croatia: assessment of Milankovitch forcing. *Sedimentary Geology* 373, 11–31.

Kemp, D.B., Van Manen, S.M., 2019. Metre-scale cycles in shallow water carbonate successions: Milankovitch and stochastic origins. *Sedimentology* 66, 2590–2604.

Koerschner, W.F., Read, J.F., 1989. Field and modelling studies of Cambrian carbonate cycles, Virginia Appalachians. *Journal of Sedimentary Petrology* 59, 654–687.

Manifold, L., Hollis, C., Burgess, P., 2020. The Anatomy of a Mississippian (Viséan) carbonate platform interior, UK: Depositional cycles, glacioeustasy and facies mosaics. *Sedimentary Geology* 401, 105633.

Ogg, J.G., Ogg, G., Gradstein, F.M., 2016. *A Concise Geological Time Scale*. Elsevier, Amsterdam.

Osleger, D.A., 1991. Subtidal carbonate cycles: implication for allocyclic versus autocyclic controls. *Geology* 19, 917–920.

Pomoni-Papaioannou, F., Kostopoulou, V., 2008. Microfacies and cycle stacking pattern in Liassic peritidal carbonate platform strata, Gavrovo-Tripolitza platform, Peloponnesus, Greece. *Facies* 54, 417–431.

Pomoni-Papaioannou, F., Karakitsios, V., 2016. Sedimentary facies analysis of a high-frequency, small-scale, peritidal carbonate sequence in the Lower Jurassic of the

Tripolis carbonate unit (central western Crete, Greece): Long-lasting emergence and fossil laminar dolocretes horizons. *Journal of Palaeogeography* 5, 241–257.

Prados, G., Bádenas, B., 2015. Sedimentary factors controlling thickness of laminated stromatolites, from laminae to metre-thick packages (Sinemurian, Iberian Basin).

*Revista de la Sociedad Geológica de España* 28, 3–14.

Pratt, B.R., James, N.P., 1986. The St George Group (Lower Ordovician) of western Newfoundland: tidal flat island model for carbonate sedimentation in shallow epeiric seas. *Sedimentology* 33, 313–343.

Pratt, B.R., James, N.P., Cowan, C.A., 1992. Peritidal carbonates. In: Walker, R.G., James, N.P., (Eds), *Facies Models: Response to Sea Level Change*. Geological Association of Canada, pp. 303–322.

Prescott, D.M., 1988. The geochemistry and palaeoenvironmental significance of iron pisoliths and ferromanganese crusts from the Jurassic of Majorca, Spain. *Eclogae Geologicae Helveticae* 81, 387–414.

Preto, N., Hinnov, L.A., De Zanche, V., Mietto, P., Hardie, L.A., 2004. The Milankovitch interpretation of the Latemar platform cycles (Dolomites, Italy): Implications for geochronology, biostratigraphy, and Middle Triassic carbonate accumulation. In: *Cyclostratigraphy: Approaches and Case Histories*. SEPM Special Publication 81, 167–182.

Rosales, I., Barnolas, A., Goy, A., Sevillano, A., Armendáriz, M., López-García, J.M., 2018. Isotope records (C-O-Sr) of late Pliensbachian-early Toarcian environmental perturbations in the westernmost Tethys (Majorca Island, Spain). *Palaeogeography Palaeoclimatology Palaeoecology* 497, 168–185.

Sadler, P.M., 1981. Sediment accumulation rates and the completeness of stratigraphic sections. *Journal of Geology* 89, 569–584.

Sadler, P.M., 1994. The expected duration of upward-shallowing peritidal carbonate cycles and their terminal hiatuses. *Geological Society of America Bulletin* 106, 791–802.

Belkhedim, S., Jarochowska, E., Benhamou, M., Nemra, A., Sadjji, R., Munnecke, A., 2019. Interplay of autogenic and allogenic processes on the formation of shallow carbonate cycles in a synrift setting (Lower Pliensbachian, Traras Mountains, NW Algeria). *Journal of Sedimentary Research* 89, 784–807.

Sames, B., Wagreich, M., Wendler, J.E., Haq, B.U., Conrad, C.P., Melinte-Dobrinescu, M.C., Hu, X., Wendler, I., Wolfgring, E., Yilmaz, I.O., Zorina, S.O., 2016. Short-term sea-level changes in a greenhouse world - A view from the Cretaceous.

*Palaeogeography, Palaeoclimatology, Palaeoecology* 441, 393–411.

Scotese, C.R., Schettino, A., 2017. Late Permian-Early Jurassic Paleogeography of Western Tethys and the World. In: *Permo-Triassic Salt Provinces of Europe, North Africa and the Atlantic Margins*, Elsevier, pp. 57–95.

Septfontaine, M., 1984. Biozonation (a l'aide des Foraminifères imperforés) de la plateforme interne carbonatée liasique du Haut Atlas (Maroc). *Revue de Micropaléontologie* 27, 209–229.

Sevillano, A., Bádenas, B., Rosales, I., Barnolas, A., López-García, J.M., 2013. Facies y secuencias de la plataforma carbonatada somera sinemuriense en la isla de Mallorca (Sección Es Barraca), España. *Geogaceta* 54, 15–18.

Sevillano, A., Rosales, I., Bádenas, B., Barnolas, A., López-García, J.M., 2019. Spatial and temporal facies evolution of a Lower Jurassic carbonate platform, NW Tethyan margin (Mallorca, Spain). *Facies* 65, 3.

Sevillano, A., Septfontaine, M., Rosales, I., Barnolas, A., Bádenas, B., López-García, J.M., 2020. Lower Jurassic benthic foraminiferal assemblages from shallow-marine platform carbonates of Mallorca (Spain): stratigraphic implications. *Journal of Iberian Geology* 46, 77–99.

Strasser, A., 1991. Lagoonal-peritidal sequences in carbonate environments: autocyclic and allocyclic processes. In: Einsele, G., Ricken, W., Seilacher, A. (Eds.), *Cycles and Events in Stratigraphy*. Springer, Heidelberg, pp. 709–721.

Strasser, A., Pittet, B., Hillgärtner, H., Pasquier, J.B., 1999. Depositional sequences in shallow carbonate-dominated sedimentary systems: concepts for a high-resolution analysis. *Sedimentary Geology* 128, 201–221.

Strasser, A., Hilgen, F.J., Heckel, P.H., 2006. Cyclostratigraphy e concepts, definitions, and applications. *Newsletters on Stratigraphy* 42, 75–114.

Strasser, A., 2018. Cyclostratigraphy of shallow-marine carbonates- Limitations and opportunities. In: Montenari, M. (Ed), *Stratigraphy and timescales 3*. Elsevier, Amsterdam, pp. 151–187.

Thierry, J., 2000. Late Sinemurian (193–191 Ma). In: Dercourt, J., Gaetani, M., Vrielynck, B., Barrier, E., Biji-Dubal, B., Brunet, M.F., Cadet, J.P., Crasquin, S., Sandulescu, M. (Eds), *Atlas Peri-Tethys. Palaeogeographical Maps—explanatory notes*. Commission for the Geologic Map of the World, Paris, pp. 49–59.



Velić, I., 2007. Stratigraphy and palaeobiogeography of Mesozoic benthic foraminifera of the Karst Dinarides (SE Europe). *Geologia Croatica* 60, 1–113.

Walkden, G.M., De Matos, J., 2000. ‘Tuning’ high frequency cyclic carbonate platform successions using omission surfaces: Lower Jurassic of the UAE and Oman. In: AlSharhan, A.S., Scott, R.W. (Eds), *Middle East Models of Jurassic/Cretaceous Carbonate Systems*. SEPM Special Publication 69, pp. 37–52.

Wilkinson, B.H., Drummond, C.N., Diedrich, N.W., Rothman, E.D., 1999. Poisson processes of carbonate accumulation on Paleozoic and Holocene platforms. *Journal of Sedimentary Research* 69, 338–350.

Yang, W., Lehrmann, D.J., Hu, X.F., 2014. Peritidal carbonate cycles induced by carbonate productivity variations: A conceptual model for an isolated Early Triassic greenhouse platform in South China. *Journal of Palaeogeography* 3, 115–126.

Zühlke, R., Bechstadt, T., Mundil, R., 2003. Sub-Milankovitch and Milankovitch forcing on a model Mesozoic carbonate platform—the Latemar (Middle Triassic, Italy). *Terra Nova* 15, 69-80.

Zühlke, R., 2004. Integrated cyclostratigraphy of a model Mesozoic carbonate platform—the Latemar (Middle Triassic, Italy). In: D’Argenio, B., Fischer, A.G., Silva, I.P., Weisert, H., Ferreri, V. (Eds.). *Cyclostratigraphy: Approaches and Case Histories*. SEPM Special Publication 81, pp. 183–211.

## FIGURE CAPTIONS

**Figure 1.** (A) Paleogeographical location of the study area in the Balearic realm in the western Tethys during the Sinemurian-earliest Pliensbachian (modified from Dercourt et al., 2000). (B) Simplified geological map of Mallorca with the location of the four studied stratigraphic sections (distance between sections without restoring the tectonic shortening). (C) Chronostratigraphic distribution of the Hettangian to Pliensbachian lithostratigraphic units in Mallorca (from Álvaro et al., 1989). The platform stages defined by Sevillano et al. (2019) within the Es Barraca Member include the platform Stage 1 studied here. Yellow bars represent the chronostratigraphic distribution of the four studied sections.

**Figure 2.** Stratigraphic logs of the peritidal to shallow subtidal platform carbonates of Stage 1 (Es Barraca Member) in the four studied sections, with distribution of the facies types based on Sevillano et al. (2019). The long-term T-R facies cycle of Stage 1 and the large-scale sequences interpreted in this work are also indicated. Location of benthic foraminifera biozones A and B is based on Sevillano et al. (2020).

**Figure 3.** Conceptual sedimentary facies model for the studied peritidal to shallow subtidal platform carbonates (Stage-1 of the Es Barraca Member; modified from Sevillano et al., 2019).

**Figure 4.** Field (a–c) and thin-section images (d–k, plane-polarized light) of lithofacies of the studied peritidal to shallow subtidal platform carbonates. (a) Supratidal flat-pebble breccia (facies 1A), with clasts made of microbial laminite. (b) Supratidal wavy-crinkled microbial laminate (facies 1B). (c) Intertidal parallel microbial laminite (facies 1C), with the alternation of micritic laminae (darker lamination) and grain-supported laminae (lighter lamination). (d) Intertidal spongiostrome stromatolite (facies 2B). Notice irregular lamination and well-developed fenestral porosity. Red arrows indicate

the presence of *Thaumatoporella parvovesiculifera* in the peloidal-bioclastic laminae. **e** Intertidal coarse-grained agglutinated stromatolite (facies 2C) with alternating dense micrite laminae (black colour) and peloidal laminae with fenestral porosity. **(f)** Intertidal fenestral mudstone (facies 2D). Red arrows indicate examples of geopetal infill of the fenestral porosity. **(g)** Intraclastic-bioclastic-peloidal grainstone (facies 3) representing sand beach sediments. **h** Oolitic-peloidal grainstone of inner bars (facies 5A). **(i)** Peloidal-intraclastic-foraminiferal grainstone (facies 5B) of inner bars, including fragments of *Thaumatoporella parvovesiculifera* (Th) and abundant small foraminifera (red arrows). **(j)** Example of skeletal wackestone (facies 6) with *Palaeodasycladus mediterraneus* (yellow arrows) and lituolids (red arrows). **(k)** Foraminiferal-peloidal-oncolitic wackestone-packstone (facies 6). Arrows show the presence of oncoids.

**Figure 5.** Interpretation of the high-frequency depositional sequences defined in this study at three different scales. Correlation of large-scale sequence 1 to 8 and their medium-scale sequences along the four studied sections. Small-scale sequences are also indicated but not correlated. For facies colour codes see Fig. 3.

**Figure 6.** Example of the large-scale sequence LS-2 in Cuevas the Artà section and field images of medium-scale sequences 2.3 and upper part of 2.5. For facies colour codes see Fig. 3.

**Figure 7.** Example of the large-scale sequence LS-7 in Cutri section and their medium- and small-scale sequences, with photographs of their field outcrop aspects. For facies colour codes see Fig. 3.

**Figure 8.** To the left, idealized complete small-scale sequences identified from the studied carbonate platform, with shallowing-upward facies trends evolving from subtidal to intertidal and finally supratidal environments. These sequences come from

the different types of small-scale sequences recognized in the studied successions (to the right). Note that these sequences are incomplete and correspond to both subtidal and peritidal sequences with gradual facies changes, except some sequences including sharp facies changes (mainly related to inner bar facies: see explanation in text).

**Figure 9.** Correlation of large-scale sequences 1 to 8 and their constituent medium-scale sequences along the four sections studied, indicating the: accumulation rates of large-scale sequences (green numbers) across the different four sections (obtained considering thickness without decompaction and a mean duration of ~400 kyr for each large-scale sequence); the number of small-scale sequences included in medium-scale sequences and the mean duration of the small-scale sequences (calculated considering a duration of ~100 kyr for each medium-scale sequence).

**Table 1.** Average thickness and minimum-maximum thickness values for the large-, medium- and small-scale sequences. Number of medium- and small-scale sequences is also indicated.

**Table 2.** Comparison of the results about factors controlling the cyclicity in this work with other studies in similar Lower Jurassic carbonate platforms in the western Tethys. The terms cycles and/or sequences (in column “scale and thickness of sequences”) has been used like they are in the original references.

Table 1

									THICKNESS (average)	THICKNESS (minimum- maximum)
LARGE-SCALE	LS-1	LS-2	LS-3	LS-4	LS-5	LS-6	LS-7	LS-8	16.5 m	10-30 m
NUMBER OF MEDIUM-SCALE SEQUENCES within L-S sequences	(3)-5	5	4	5	(3)-5	(2)-4	4	(1)-3	4 m	1-10 m
NUMBER OF SMALL-SCALES SEQUENCES within M-S sequences	1-8	1-6	1-17	1-8	1-9	1-11	1-16	1-6	1 m	0.3-5 m

Table 2

<b>Lower Jurassic peritidal - shallow carbonate platforms in western Tethys</b>					
REFERENC E	LOCATION / Age	SCALE AND THICKNESS OF SEQUENCES	Alloccyclic processes		Autocycli c processe s
			EUSTASY - Orbitally driven sequences (Milankovitch band)	LOCAL OR REGIONA L TECTONI C (tectonic differential subsidence)	
Bosence <i>et al</i> , 2000	Rock of Gibraltar (Iberian Peninsula) <i>Hett. - Sinemurian</i>	high-frequency cycles (1-10 m)	✓	✓	✓
Bosence <i>et al</i> , 2009	Western tethys (Spain, Italy, Greece, Tunisia, Morocco, Gibraltar) <i>Sinemurian</i>	meter-scale cycles (1-5 m) = parasequences and high-frequency sequences	✓	✓	✓
Bádenas <i>et al</i> , 2010	Iberian Range (Spain) <i>Late Sinemurian</i>	small-scale cycles (1-8 m)	✓	✓	✓
Pomoni-Papaioannou and Kostopoulou, 2008	Gavrovo-Tripolitza platform (Greece) <i>Early-middle Lias</i>	small-scale cycles (6-7 m)	✓		
Pomoni-Papaioannou and Karakitsios, 2016	Tripolis carbonate unit (central western Creta, Greece) <i>Lower-Middle Jurassic</i>	small-scale cycles (1-10 m)	✓	✓	✓
Crevello, 1991	Central and Eastern High Atlas rift (Morocco) <i>Sinemurian-Pliensb.</i>	bundles (10-50 m) cycles (1-10 m)	✓ Obliquity Eccentricity	✓	
Brandano <i>et al</i> , 2015	Central Apennines (Italy)	high-frequency cycles (1-6)	✓ Precession?	✓	✓

	<i>Lias</i>	m), bundles (7-8 m) and super-bundles (10-30 m)	Obliquity Long/short Eccentricity		
Belkhedim <i>et al</i> , 2019	Traras Mountains, (NW Algeria) <i>lower Pliensbachian</i>	small-scale cycles (2-10 m)	✓	✓	✓
<b>THIS WORK</b>	Mallorca island, (Spain) <i>early Sinem - earliest late Sinemurian</i>	small-scale seq. (0.3-5 m)	Precession? ✓	✓	✓
		medium-scale seq. (1-10 m)	Short Eccentricity ✓	✓	
		large-scale seq. (10-30 m)	Long Eccentricity ✓	✓	



Dominant control factor



Probable control factor (it cannot be disregarded)



Journal Pre-proof

**Declaration of interests**

The authors declare that they have no known competing financial interests or personal relationships that could have appeared to influence the work reported in this paper.

The authors declare the following financial interests/personal relationships which may be considered as potential competing interests:

Journal Pre-proof



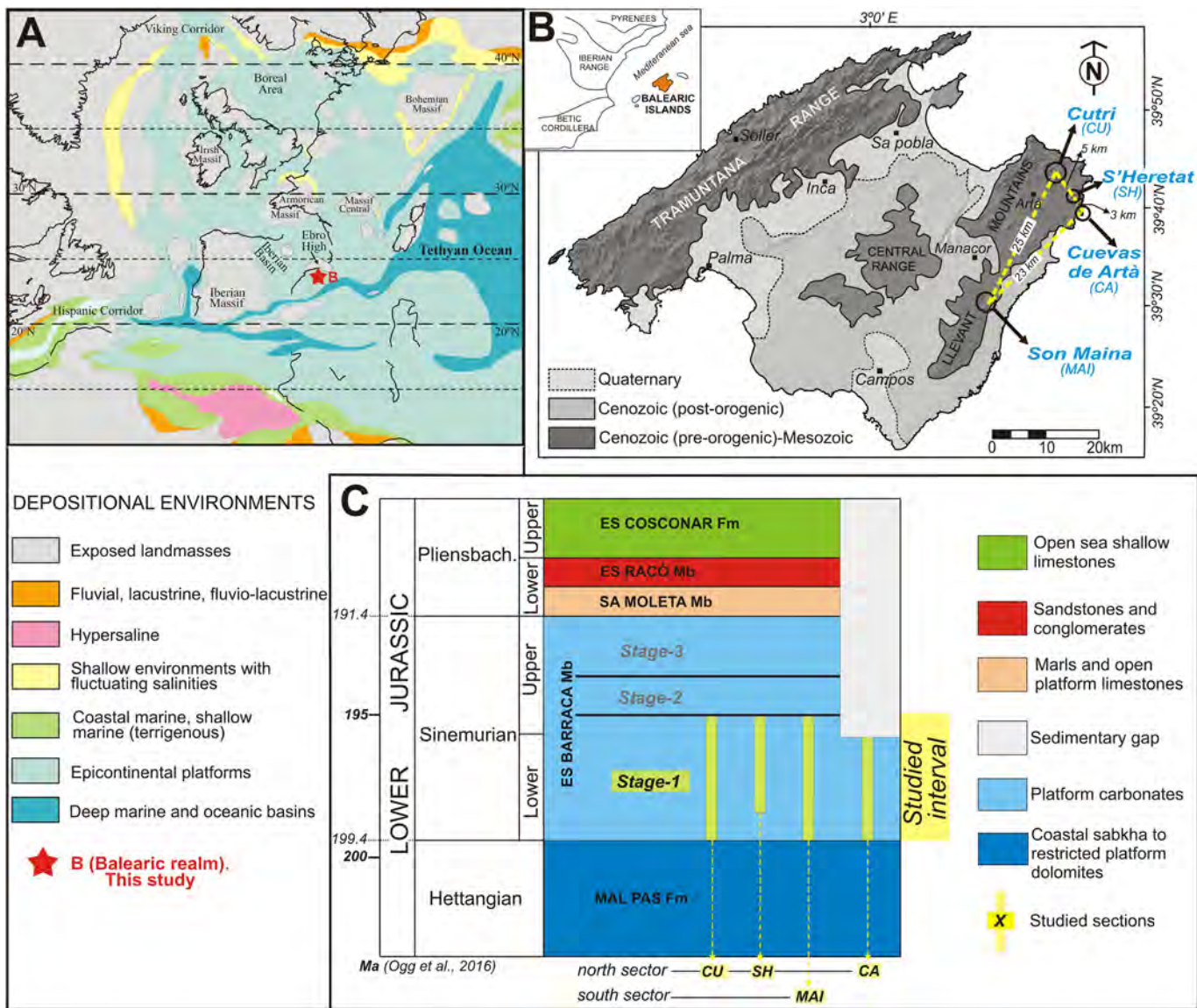


Figure 1

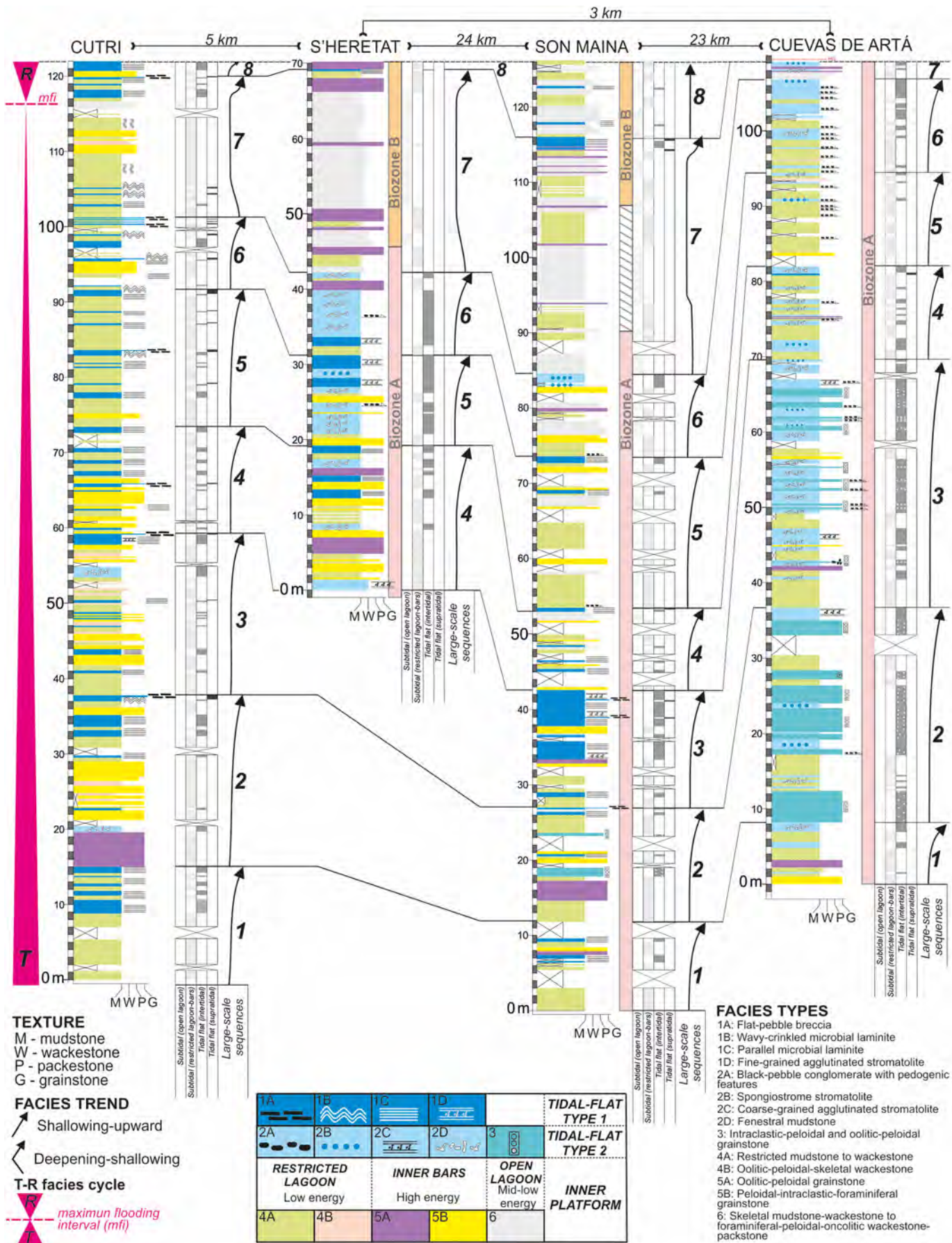




















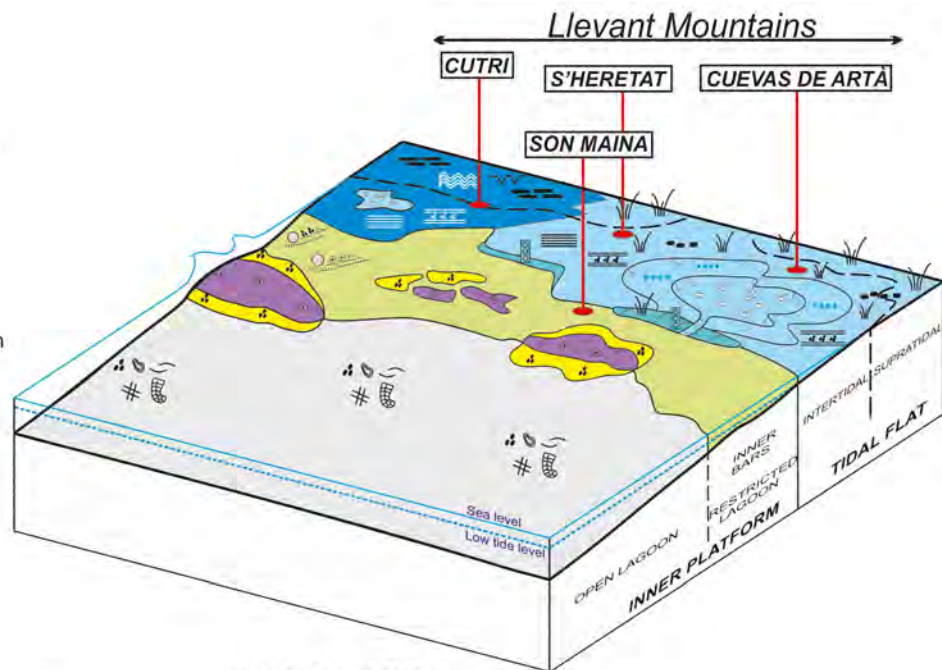


Figure 2












## Legend

-  Desiccation cracks
-  Tepees
-  Flat pebbles
-  Wavy-crinkled microbial lamination
-  Parallel microbial lamination
-  Agglutinated stromatolites
-  Spongiostrome stromatolites
-  Fenestral porosity
-  Parallel tractive lamination
-  Peloidal/ooidal tractive accumulation
-  Black pebble/intraclastic tractive accumulation
-  Intraclastic/peloidal/ooidal sands
-  Ooids
-  Peloids
-  Oncoids
-  Black pebbles
-  Dasycladalean algae
-  Bivalves
-  Foraminifera (textulariids)
-  Foraminifera (lituolids)



## FACIES ASSOCIATIONS

1A	1B	1C	1D	
				<b>TIDAL-FLAT TYPE 1</b>
				
				<b>TIDAL-FLAT TYPE 2</b>
<b>RESTRICTED LAGOON</b> Low energy		<b>INNER BARS</b> High energy		
		<b>OPEN LAGOON</b> Mid-low energy		<b>INNER PLATFORM</b>
<b>4A</b>	<b>4B</b>	<b>5A</b>	<b>5B</b>	
<b>6</b>				

## FACIES TYPES

- 1A: Flat-pebble breccia
- 1B: Wavy-crinkled microbial laminite
- 1C: Parallel microbial laminite
- 1D: Fine-grained agglutinated stromatolite
- 2A: Black-pebble conglomerate with pedogenic features
- 2B: Spongiostrome stromatolite
- 2C: Coarse-grained agglutinated stromatolite
- 2D: Fenestral mudstone
- 3: Intraclastic-peloidal and oolitic-peloidal grainstone
- 4A: Restricted mudstone to wackestone
- 4B: Oolitic-peloidal-skeletal wackestone
- 5A: Oolitic-peloidal grainstone
- 5B: Peloidal-intraclastic-foraminiferal grainstone
- 6: Skeletal mudstone-wackestone to foraminiferal-peloidal-oncolitic wackestone-packstone

Figure 3



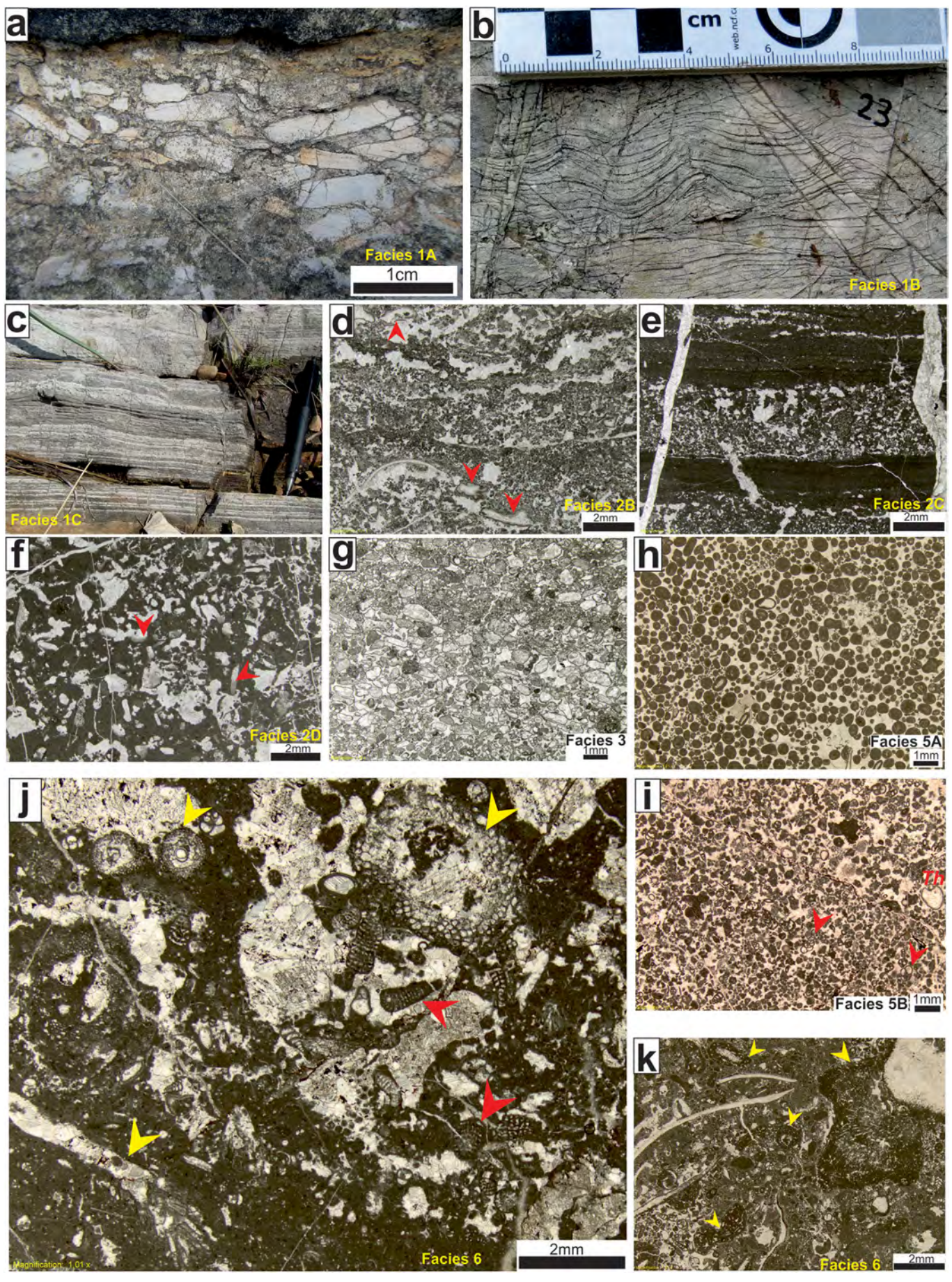


Figure 4



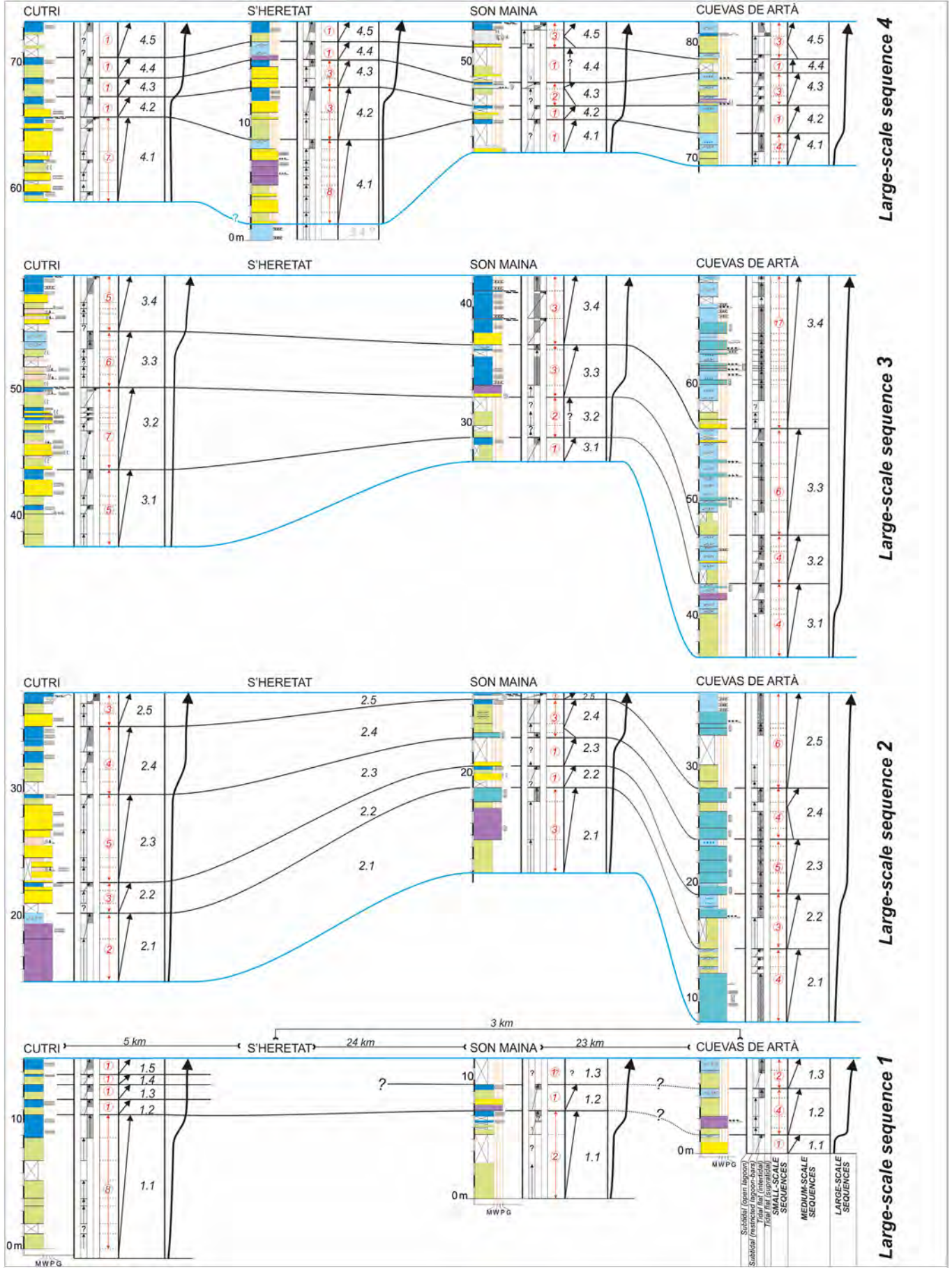


Figure 5

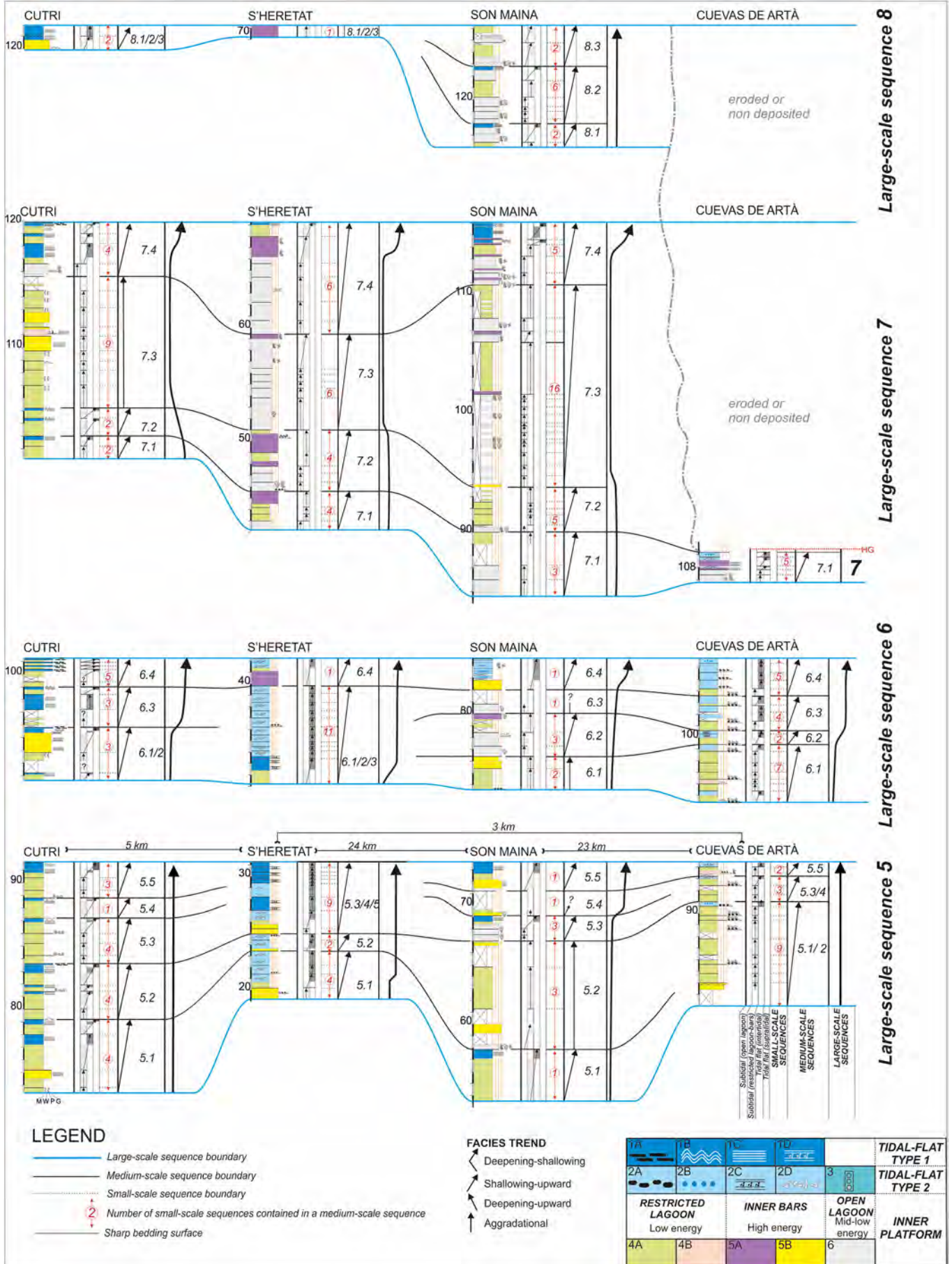
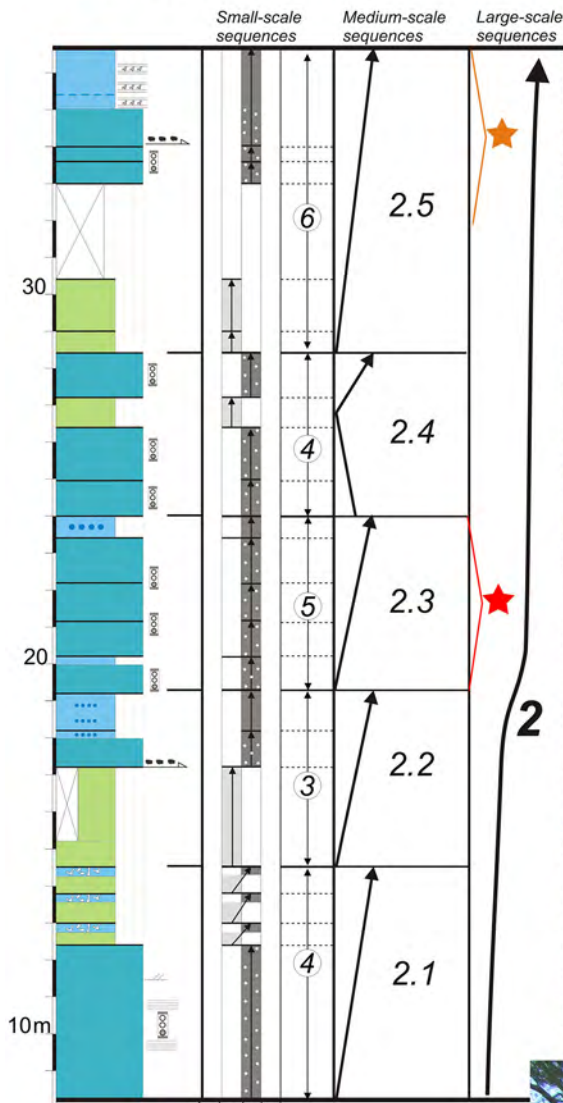


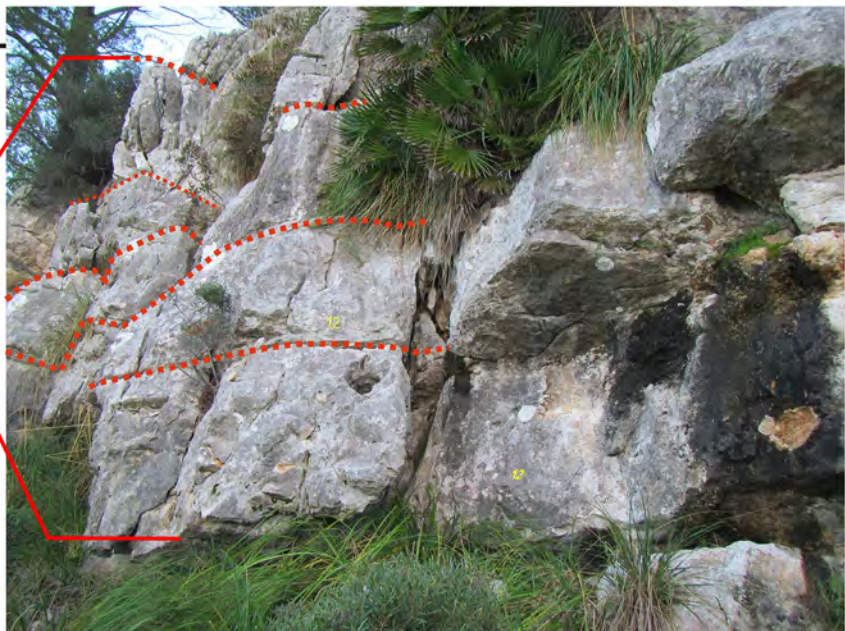
Figure 5r1



# CUEVAS DE ARTÀ SECTION



Subtidal (open lagoon)  
 Subtidal (restricted lagoon-bars)  
 Tidal flat (intertidal)  
 Tidal flat (supratidal)



**LEGEND**  
 Small-scale sequence boundary (log) -----  
 Small-scale sequence boundary (image field) .....  
 Simple bedding surface - - - - -

Figure 6



# CUTRI SECTION

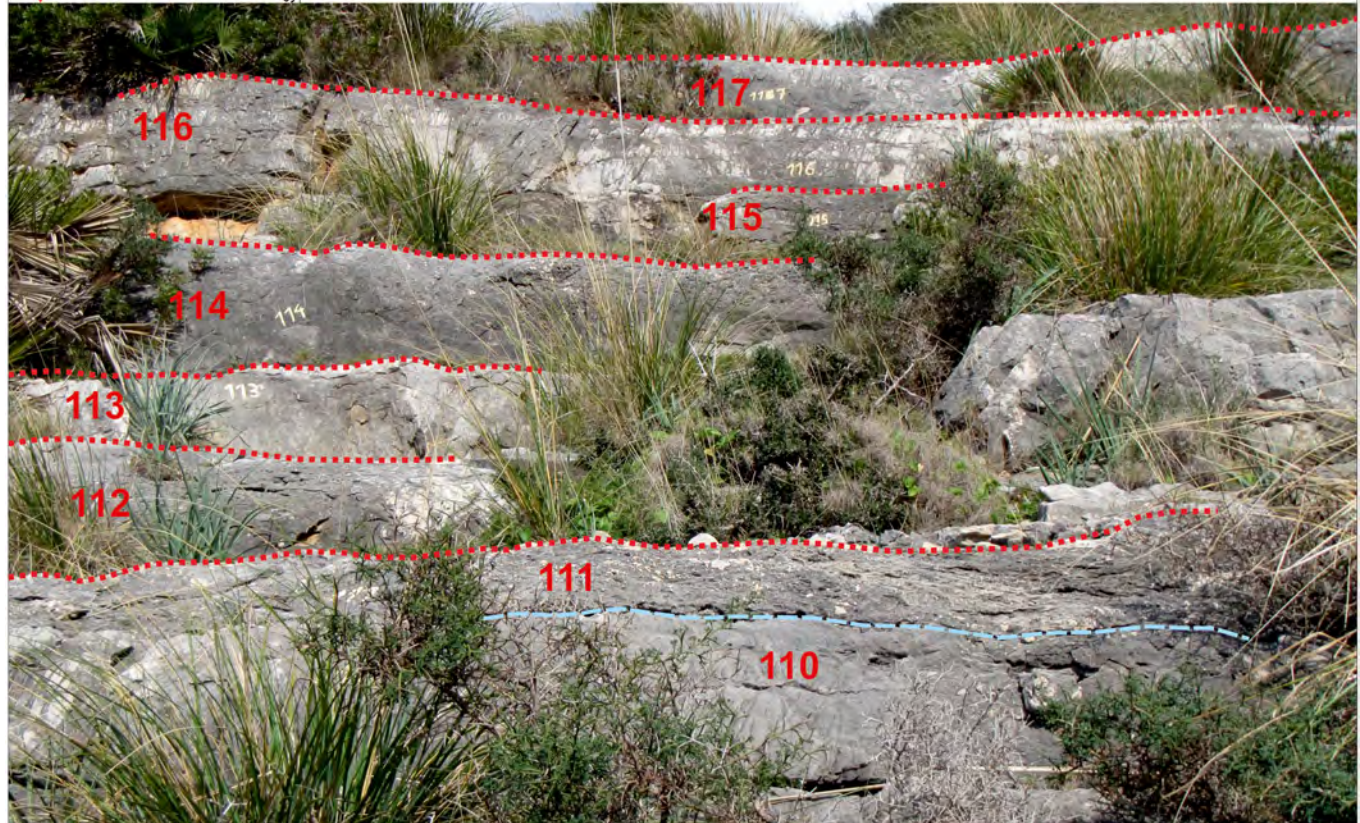
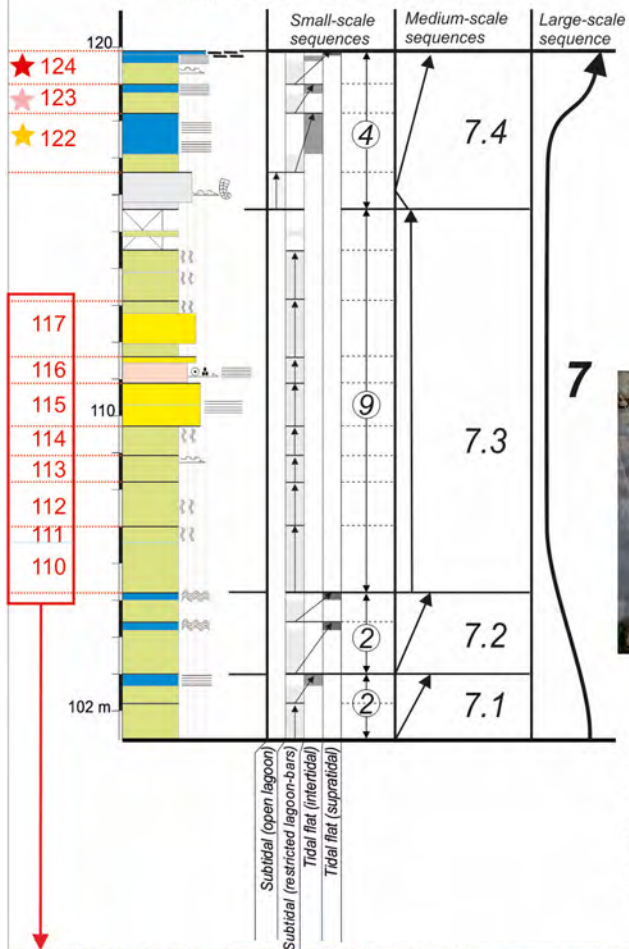
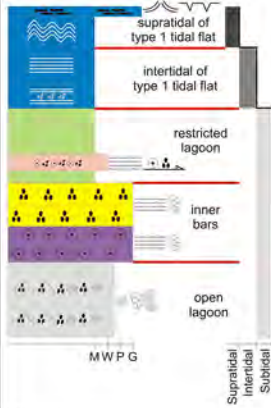


Figure 7

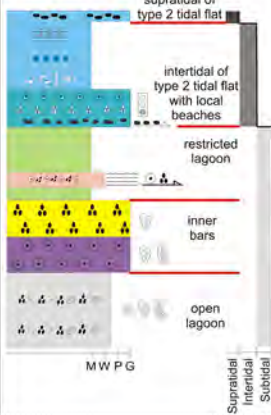


# IDEALIZED COMPLETE SMALL-SCALE SEQUENCES

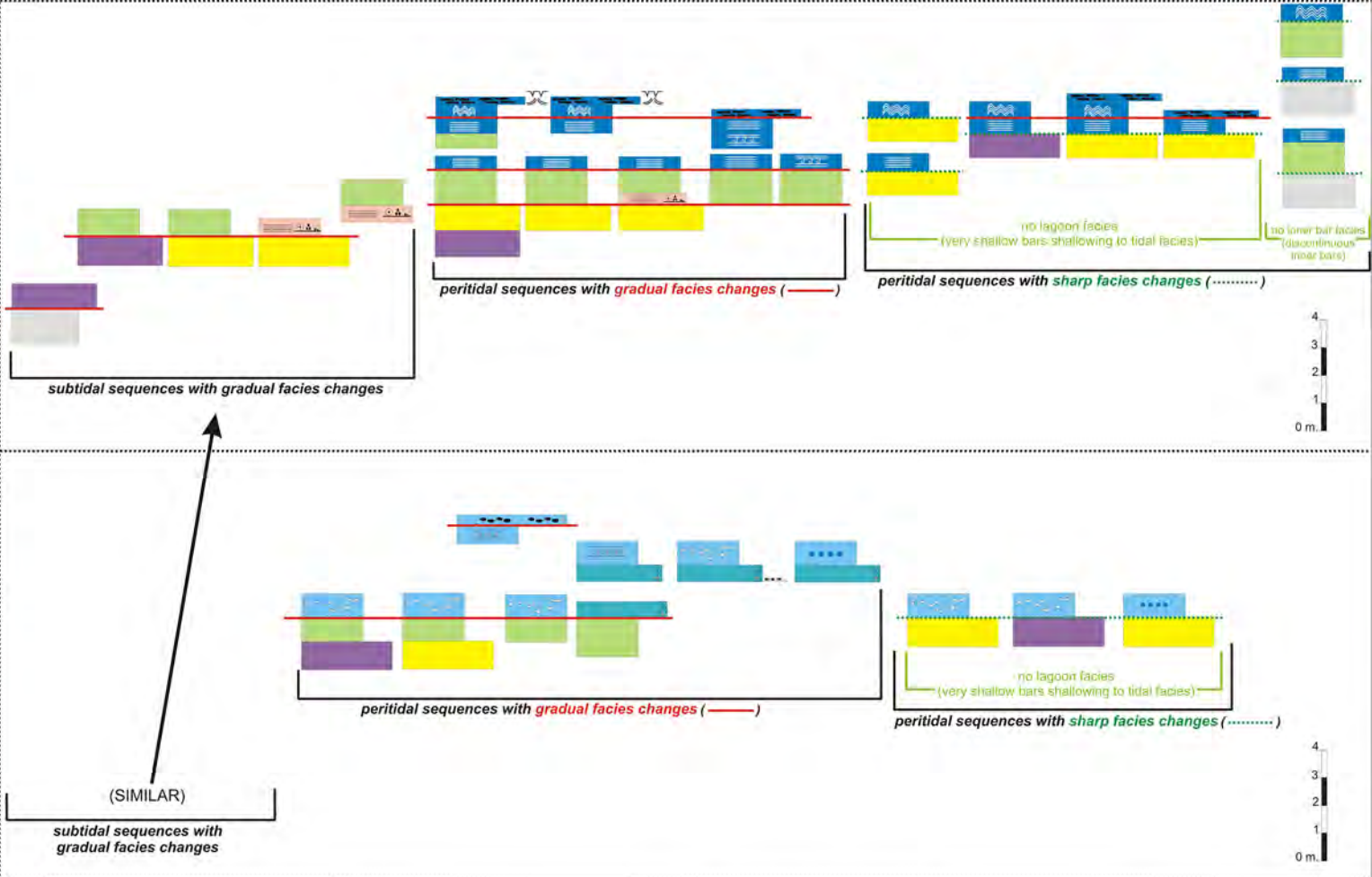
(for type 1 tidal flat)



(for type 2 tidal flat)



# SMALL-SCALE SEQUENCES RECOGNIZED



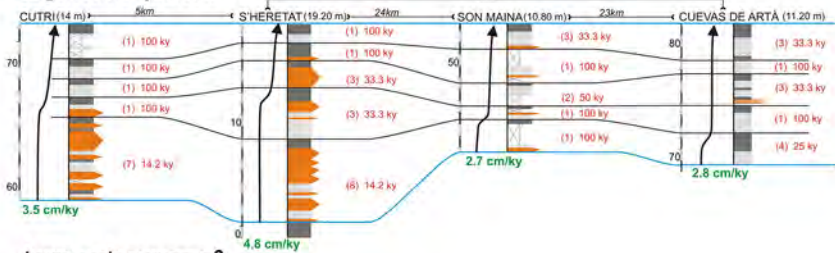
FACIES ASSOCIATIONS				
				<b>TIDAL-FLAT TYPE 1</b>
				<b>TIDAL-FLAT TYPE 2</b>
<b>RESTRICTED LAGOON</b>	<b>INNER BARS</b>	<b>OPEN LAGOON</b>	<b>INNER PLATFORM</b>	

## LEGEND

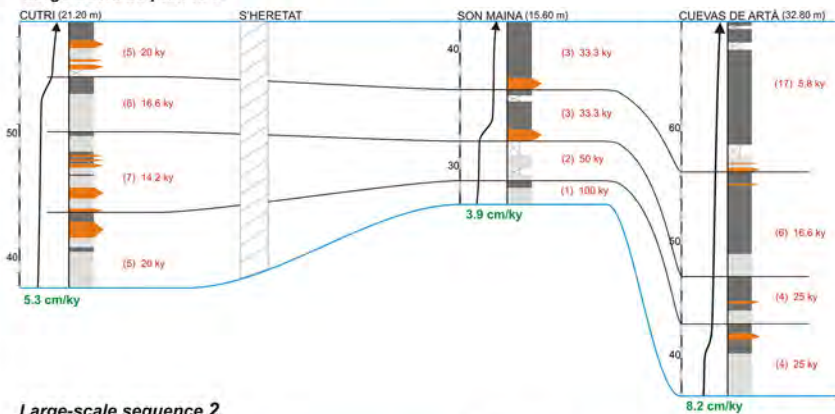
- Desiccation cracks
- Tepees
- Agglutinated stromatolites
- Spongiosome stromatolites
- Flat pebbles
- Fenestral porosity
- Wavy-crenulated microbial lamination
- Parallel tractive lamination
- Peloidal/ooidal tractive accumulation
- Black pebble/intraclastic tractive accumulation
- Intraclastic/peloidal/ooidal sands
- Ooids
- Peloids
- Oncoids
- Black pebbles
- Dasycladalean algae
- Foraminifera (textulariids)
- Foraminifera (lituolids)

Figure 8

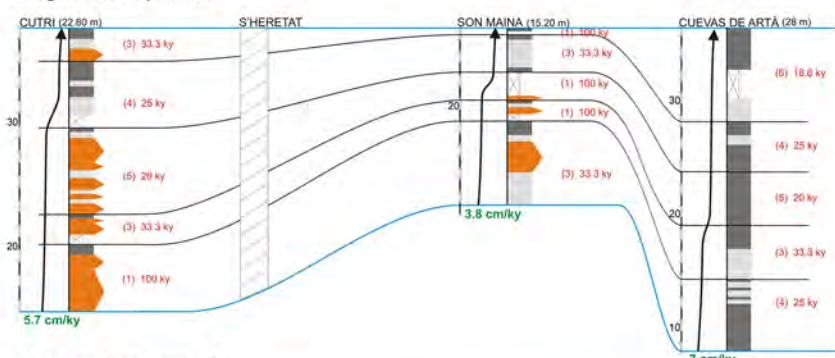
#### Large-scale sequence 4



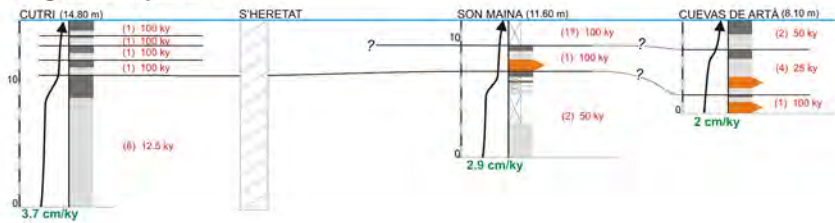
#### Large-scale sequence 3



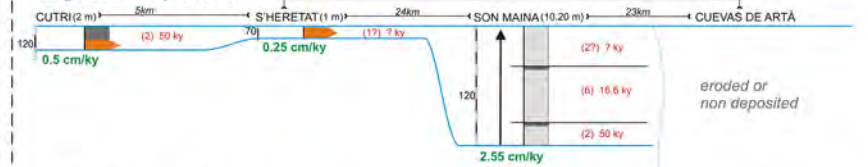
#### Large-scale sequence 2



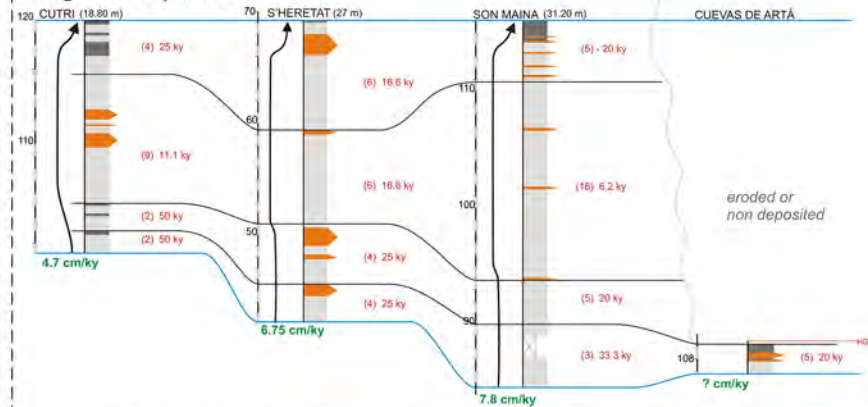
#### Large-scale sequence 1



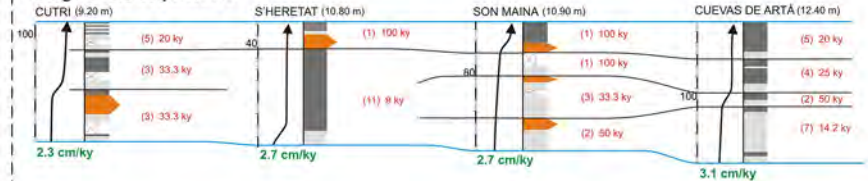
#### Large-scale sequence 8



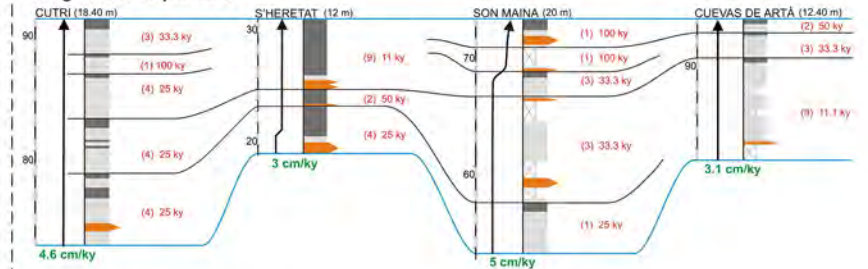
#### Large-scale sequence 7



#### Large-scale sequence 6



#### Large-scale sequence 5



#### LEGEND

- Large-scale sequence boundary
- Medium-scale sequence boundary
- X cm/ky Large-scale sequence accumulation rate
- (X) X ky (N° of small-scale sequences) Mean duration of small-scale sequences
- Inter- and supratidal facies
- Subtidal facies
- ▬ (Subtidal bars)

Figure 9